

11-1-2004

## Development of a Solid Electrolyte for Hydrogen Production

Kiran Sampat Gaikwad  
*University of South Florida*

Follow this and additional works at: <https://digitalcommons.usf.edu/etd>



Part of the [American Studies Commons](#)

---

### Scholar Commons Citation

Gaikwad, Kiran Sampat, "Development of a Solid Electrolyte for Hydrogen Production" (2004). *USF Tampa Graduate Theses and Dissertations*.

<https://digitalcommons.usf.edu/etd/1043>

This Thesis is brought to you for free and open access by the USF Graduate Theses and Dissertations at Digital Commons @ University of South Florida. It has been accepted for inclusion in USF Tampa Graduate Theses and Dissertations by an authorized administrator of Digital Commons @ University of South Florida. For more information, please contact [digitalcommons@usf.edu](mailto:digitalcommons@usf.edu).

# Development of a Solid Electrolyte for Hydrogen Production

by

Kiran Sampat Gaikwad

A thesis submitted in partial fulfillment  
of the requirements for the degree of  
Master of Science in Electrical Engineering  
Department of Electrical Engineering  
College of Engineering  
University of South Florida

Major Professor: Elias K. Stefanakos, Ph.D., P.E.  
Burton Krakow, Ph.D.  
Venkat Bhethanabotla, Ph.D.

Date of Approval:  
November 1, 2004

Keywords: solid acid electrolytes, superprotonic conductivity, impedance measurements,  
differential scanning calorimetry, x-ray diffraction, infrared spectroscopy

© Copyright 2004, Kiran Sampat Gaikwad

## **ACKNOWLEDGEMENTS**

First of all I would like to thank *Shree Siddhivinayak* and my family for giving me the strength and will to complete my work. I am grateful to Dr. Elias K. Stefanakos for being a constant source of motivation and showing his faith in me. I would also like to thank Dr. Burton Krakow for his valuable guidance without which it would not be possible to complete my work. I would like to express my sincere gratitude towards Dr. Venkat Bhethanabotla and Dr. Sagues for allowing me to use the facilities in their labs. I am highly indebted to Mr. Sesa Srinivasan for giving his time in achieving the results for my thesis. Finally, I would like to thank Amol Chaudhari, Mahesh Chettiar, Eric Weaver, Eric Todd, Alaa Kababji and Matt Smith for their help and support in my work.

## TABLE OF CONTENTS

LIST OF TABLES	iii
LIST OF FIGURES	iv
ABSTRACT	vi
CHAPTER 1 INTRODUCTION	1
1.1 Introduction	1
1.2 Electrolyte	2
1.3 Solid Electrolytes	3
1.4 Solid Acid Electrolytes	3
1.4.1 Properties of Solid Acid Electrolytes	4
1.4.2 Benefits of Solid Acid Electrolytes	5
1.5 Organization of Thesis	5
CHAPTER 2 LITERATURE REVIEW	6
2.1 California Institute of Technology	6
2.2 The University of Texas at Austin	7
CHAPTER 3 THEORY OF SOLID ACIDS	9
3.1 Structure	9
3.1.1 Atomic Bonding	9
3.1.2 Hydrogen Bonding	10
3.1.2.1 Intra-Hydrogen Bonds	11
3.1.2.2 Inter-Hydrogen Bonds	13
3.2 Coordination	14
3.3 Order-Disorder	14
3.3.1 Dynamic Disorder	15
3.3.2 Intra-Hydrogen Bond Disorder	15
3.3.3 Inter-Hydrogen Bond Disorder	16
3.3.4 Oxy-anion Disorder	16
3.4 Properties	16
3.4.1 Ionic Conductivity	16
3.4.2 Protonic Conductivity	20
3.4.2.1 Atomic Diffusion	20
3.4.2.2 Proton Displacement	20
3.4.2.3 Molecular Reorientation	20
3.4.2.4 Vehicle Mechanism	21
3.4.2.5 Grotthus Mechanism	21

3.5	Phase Transitions	21
3.5.1	General Characterization	22
3.5.2	High Temperature Proton Conduction in Solid Acids	23
CHAPTER 4	DESIGN AND DEVELOPMENT OF SOLID ACID ELECTROLYTE	24
4.1	CsHSO <sub>4</sub> Prepared from Equimolar Amounts of Cs <sub>2</sub> SO <sub>4</sub> and H <sub>2</sub> SO <sub>4</sub>	24
4.2	CsHSO <sub>4</sub> Prepared from Cs <sub>2</sub> CO <sub>3</sub> and H <sub>2</sub> SO <sub>4</sub> such that Cs <sub>2</sub> CO <sub>3</sub> : H <sub>2</sub> SO <sub>4</sub> ::1:2	25
4.3	Pellet Preparation	26
4.3.1	For 0.5" Diameter Pellet and 1 mm Thickness	26
4.3.2	For 2.0" Diameter Pellet and 1 mm Thickness	27
4.4	Die Design	28
4.4.1	Pellets of 0.5" Diameter	29
4.4.2	Pellets of 2.0" Diameter	31
CHAPTER 5	THEORY OF EXPERIMENTAL MEASUREMENTS	33
5.1	Impedance Measurement	33
5.2	Differential Scanning Calorimetry (DSC)	37
5.3	X-Ray Diffraction	38
5.4	Infrared Spectroscopy	39
CHAPTER 6	EXPERIMENTAL RESULTS	41
6.1	Impedance Measurements Results	41
6.2	Differential Scanning Calorimetry(DSC) Results	46
6.3	X-Ray Diffraction Results	49
6.3.1	Anchor Scan Parameters	49
6.3.2	X-Ray Diffraction Pattern of CsHSO <sub>4</sub>	50
6.3.3	Peak List	50
6.3.4	Identified Patterns List	51
6.3.5	Plot of Identified Phases	52
6.4	Infrared Spectroscopy Results	52
CHAPTER 7	SUMMARY AND CONCLUSIONS	54
CHAPTER 8	RECOMMENDATIONS FOR FUTURE WORK	56
REFERENCES		57

## LIST OF TABLES

Table 1.1 Comparison of Electronic and Ionic Conductivity	2
Table 3.1 Correlation Between Hydrogen Bond Types and Bond Character	11
Table 3.2 Effects of Symmetry on Strong, Medium and Weak Hydrogen Bonds	12
Table 3.3 Inter-Hydrogen Bond Networks Exhibited by CsHSO <sub>4</sub> Solid Acid	13
Table 4.1 Amount of Force Required to Press Discs of Different Diameters	28
Table 4.2 Specifications of Die, Punch and Base	29
Table 6.1 Impedance Measurements Results	45
Table 6.2 DSC Results	49
Table 6.3 Peak List for the X-Ray Diffraction Pattern of CsHSO <sub>4</sub>	50
Table 6.4 Identified Patterns List for the X-Ray Diffraction Pattern of CsHSO <sub>4</sub>	51

## LIST OF FIGURES

Fig 4.1 0.5” Diameter Pellets of CsHSO <sub>4</sub>	27
Fig 4.2 2.0” Diameter Pellets of CsHSO <sub>4</sub>	28
Fig 4.3 Design of Punch, Die and Base for Preparing 0.5” Diameter Pellets	29
Fig 4.4 Fabricated Punch, Die and Base for Preparing 0.5” Diameter Pellets	30
Fig 4.5 Hydraulic Press Used for Preparing 0.5” Diameter Pellets	30
Fig 4.6 Design of Punch, Die and Base for Preparing 2.0” Diameter Pellets	31
Fig 4.7 Fabricated Punch, Die and Base for Preparing 2.0” Diameter Pellets	31
Fig 4.8 MTS Press Used for Preparing 0.5” Diameter Pellets	32
Fig 5.1 Time Dependent Wave Function	34
Fig 5.2 Nyquist Plot of the AC Impedance of a Material as a Function of Frequency $\omega$	36
Fig 5.3 Equivalent RC Circuit	36
Fig 5.4 Differential Scanning Calorimetry Setup	37
Fig 6.1 Log[ $\sigma$ ] v/s T for 0.5” Dia. Pellet of CsHSO <sub>4</sub> from CS <sub>2</sub> CO <sub>3</sub> with Ag Paste	41
Fig 6.2 Log[ $\sigma$ ] v/s T for 0.5” Dia. Pellet of CsHSO <sub>4</sub> from CS <sub>2</sub> CO <sub>3</sub> without Ag Paste	42
Fig 6.3 Log[ $\sigma$ ] v/s T for 2.0” Dia. Pellet of CsHSO <sub>4</sub> from CS <sub>2</sub> CO <sub>3</sub> with Ag Paste	42
Fig 6.4 Log[ $\sigma$ ] v/s T for 2.0” Dia. Pellet of CsHSO <sub>4</sub> from CS <sub>2</sub> CO <sub>3</sub> without Ag Paste	43
Fig 6.5 Log[ $\sigma$ ] v/s T for 0.5” Dia. Pellet of CsHSO <sub>4</sub> from CS <sub>2</sub> SO <sub>4</sub> with Ag Paste	43
Fig 6.6 Log[ $\sigma$ ] v/s T for 0.5” Dia. Pellet of CsHSO <sub>4</sub> from CS <sub>2</sub> SO <sub>4</sub> without Ag Paste	44
Fig 6.7 Log[ $\sigma$ ] v/s T for 2.0” Dia. Pellet of CsHSO <sub>4</sub> from CS <sub>2</sub> SO <sub>4</sub> with Ag Paste	44

Fig 6.8 Log[ $\sigma$ ] v/s T for 2.0” Dia. Pellet of CsHSO <sub>4</sub> from CS <sub>2</sub> SO <sub>4</sub> without Ag Paste	45
Fig 6.9 DSC Plot of CsHSO <sub>4</sub>	46
Fig 6.10 DSC Plot of Barium Hydrogen Phosphate	47
Fig 6.11 DSC Plot of Barium Dihydrogen Phosphate	47
Fig 6.12 DSC Plot of Cesium Hydrogen Carbonate	48
Fig 6.13 DSC Plot of Ammonium Iodide	48
Fig 6.14 X-Ray Diffraction Pattern of CsHSO <sub>4</sub>	50
Fig 6.15 Plot of Identified Phases	52
Fig 6.16 Infrared Spectroscopy Results of CsHSO <sub>4</sub> made from Cesium Sulfate	52
Fig 6.17 Infrared Spectroscopy Results of CsHSO <sub>4</sub> made from Cesium Carbonate	53



# **DEVELOPMENT OF A SOLID ELECTROLYTE FOR HYDROGEN PRODUCTION**

Kiran Sampat Gaikwad

## **ABSTRACT**

Electrolytic cells convert chemical energy directly into electrical energy cleanly and efficiently. An integral component of a fuel cell and an electrolytic cell is the electrolyte, a material that conducts ions. Liquid electrolytes can be aqueous as in the phosphoric acid and alkaline fuel cells, or molten, as in the molten carbonate fuel cells. A solid electrolyte is preferable because it allows sturdier, more efficient and corrosion resistant systems to be built.

The main objective of this work is to develop a solid electrolyte for hydrogen production by electrolysis of hydrogen sulfide. Barium Hydrogen Phosphate, Barium Dihydrogen Phosphate, Cesium Hydrogen Carbonate, and Ammonium Iodide received brief attention but Cesium Hydrogen Sulfate was the primary candidate considered. Initial investigation has verified that Cesium Hydrogen Sulfate undergoes an impressive first-order phase transition at approximately 140°C at which the proton conductivity increases by almost four orders of magnitude. An electrochemical cell was designed and developed by Erik Todd for the production of hydrogen. Hydrogen sulfide can electrolyzed into hydrogen and sulfur in an electrochemical cell. Sulfur is in a low viscosity molten state at a temperature of 150°C. A cell with cesium hydrogen sulfate electrolyte can operate at this temperature where liquid sulfur and gaseous hydrogen can

move out of the cell as they are formed. Consequently, the electrolyte must possess a high conductivity at this temperature to facilitate the migration of hydrogen ions to the negative electrode through the electrolyte. Cesium Hydrogen Sulfate is known to act as an insulator at room temperature and a protonic conductor at 140°C. Hence it comes as an obvious choice as an electrolyte in a hydrogen sulfide electrochemical cell. The structural and chemical properties of Cesium Hydrogen Sulfate were investigated.

- The CsHSO<sub>4</sub> electrolyte was prepared by the reaction of cesium carbonate and cesium sulfate with sulfuric acid respectively.
- A punch, die and base were designed and fabricated to make 0.5” and 2.0” diameter pellets for that purpose.
- X-ray diffraction was performed on the 0.5” diameter pellets to identify and characterize the polycrystalline phases of the solid acid electrolyte.
- Differential Scanning Calorimetry was performed so as to ascertain the phase transition temperature.
- The temperature at which the phase transition occurs was further confirmed by impedance measurements. A test setup was built in order to perform impedance measurements. An experiment to measure the impedance of a 0.5” diameter pellet of silver iodide was performed in order to test the validity of the setup.
- An infrared analysis was performed on the prepared sample of CsHSO<sub>4</sub> in order to identify the bond environment of the electrolyte.
- Differential scanning calorimetry was performed with Barium Hydrogen Phosphate, Barium Dihydrogen Phosphate, Cesium Hydrogen Carbonate and Ammonium Iodide to identify their phase transition temperatures.

- A successful electrolysis of steam experiment was carried out using the  $\text{CsHSO}_4$  electrolyte to evaluate its performance.
- Finally, the  $\text{CsHSO}_4$  electrolyte was tested in the hydrogen sulfide electrochemical cell for the production of hydrogen and sulfur.

# CHAPTER 1

## INTRODUCTION

### 1.1 Introduction

Hydrogen has the potential to solve major challenges facing America today namely dependence on petroleum imports, poor quality of air and greenhouse gas emissions. Currently, the National Aeronautics and Space Administration (NASA) utilize hydrogen as a fuel for launching shuttles to space from the Kennedy Space Center at Cape Canaveral, Florida. The source of hydrogen for this purpose comes from natural gas produced in New Orleans and Texas. Each shuttle launch consumes approximately 300,000 pounds of hydrogen which evidently needs to be transported from New Orleans or Texas to Cape Canaveral, Florida. Considering the economics of the task NASA spends a large amount of money in transportation of hydrogen from the production site to the launch site. These high costs can be reduced considerably if a technology to produce hydrogen at or near the launch site can be developed. Moreover hydrogen being a clean and environmentally friendly fuel it can be used in Florida in other applications.

In this work the electrolysis of hydrogen sulfide to produce hydrogen and sulfur is considered. Hydrogen sulfide, being a toxic waste emitted from many industrial processes it would be available in abundance. Liquid sulfur has a low viscosity at a temperature of 150°C. Electrolysis of hydrogen sulfide would facilitate the removal of the sulfur product from the cell. Hence, the need for a solid electrolyte having a high

conductivity at 150°C. Cesium Hydrogen Sulfate undergoes an impressive first-order phase transition at 140-150°C at which the proton conductivity increases by almost four orders of magnitude. The main purpose of this work is to investigate the use of Cesium Hydrogen Sulfate electrolyte for application in hydrogen sulfide electrochemical cells. Since Barium Hydrogen Phosphate, Barium Dihydrogen Phosphate, Cesium Hydrogen Carbonate, Ammonium Iodide are known to have a similar structure as that of Cesium Hydrogen Sulfate it is therefore important to investigate the properties of these compounds for consideration.

## 1.2 Electrolyte

An electrolyte may be defined as an electric conductor in which current is carried by the movement of ions. Most electrolytes are liquids, but some electrolytes are solids. [1]

The following table shows the difference between ionic conductivity and electronic conductivity:

Table 1.1 Comparison of Electronic and Ionic Conductivity [1]

Electronic Conductivity	Ionic Conductivity
Conductivity range $10 \text{ S/cm} < \sigma < 10^5 \text{ S/cm}$	Conductivity range $10^{-3} \text{ S/cm} < \sigma < 10 \text{ S/cm}$
Electrons carry current	Ions carry current
Conductivity increases as temperature decreases	Conductivity decreases as temperature decreases

### 1.3 Solid Electrolytes

Solid ionic electrolytes generally exhibit the following characteristics:

- A large number of the ions of one species should be mobile in the electrolyte. This requires a large number of empty sites, either vacancies or accessible interstitial sites. Empty sites are required for ions to move through the lattice.
- The empty and occupied sites should have similar potential energies with a low activation energy barrier for jumping between neighboring sites. A high activation energy decreases carrier mobility. Very stable sites (deep potential energy wells) lead to carrier localization.
- The structure of the electrolyte should have solid framework, preferably 3D, permeated by open channels. The migrating ion lattice should be “molten”, so that a solid framework of the other ions is needed in order to prevent the entire material from melting.
- The framework ions (usually anions) should be highly polarizable. Such ions can deform to stabilize transition state geometries of the migrating ion through covalent interactions.[1]

### 1.4 Solid Acid Electrolytes

Solid acids, or acid salts, like Cesium Hydrogen Sulfate are a class of compounds whose chemistry and properties lie between those of a normal acid e.g.,  $\text{H}_2\text{SO}_4$  and a normal salt e.g.,  $\text{K}_2\text{SO}_4$ . They usually consist of oxyanions, such as  $\text{SO}_4^{2-}$ , which are linked together by hydrogen bonds. Initial research has revealed that Cesium Hydrogen Sulfate undergoes an impressive first-order phase transition at approximately  $140^\circ\text{C}$  at

which the proton conductivity increases by almost four orders of magnitude. The increase in conductivity may be attributed to the local defects in the structure and subsequent protonic transition.

At room temperature the Cesium Hydrogen Sulfate has a monoclinic symmetry. Above the phase transition temperature, the symmetry of the compound increases and the oxygen atoms become disordered to contain the higher symmetry. The partial occupancy of the oxygen sites gives a nearly liquid-like nature to the protons as the earlier static hydrogen bonded system becomes highly dynamic. In this dynamic system, the SO<sub>4</sub> groups are rearranged with inter-tetrahedra hopping of the proton. This fast reorientation of the tetrahedra in conjunction with proton translations leads to the jump in conductivity across the phase transition and to the “superprotonic conduction” many solid acids exhibit in their high temperature phases.[2]

#### **1.4.1 Properties of Solid Acid Electrolytes**

Solid acid electrolytes exhibit the following properties:

- True solid state proton conductors
- Insulators at room temperature
- Ionic conductors above a transition temperature usually above 100°C
- Operate with no liquid water
- Modest catalyst requirements
- Waste heat is hot enough for use in domestic water heating or space conditioning as well as to generate the steam that is electrolyzed
- Impermeable to fuels and electrode scavengers

### **1.4.2 Benefits of Solid Acid Electrolytes**

The benefits of solid acid electrolytes are as follows:

- Sturdy
- Vibration and corrosion resistant
- Durable

### **1.5 Organization of Thesis**

This thesis is organized in eight chapters. The second chapter gives a brief description of a few technical papers and the background work already carried out on the  $\text{CsHSO}_4$  solid acid electrolyte. The third chapter covers the theoretical aspects of solid acid electrolytes and provides detailed information on the reasons for the superprotonic phase transition of  $\text{CsHSO}_4$  solid acids. The development of a solid acid electrolyte is described in chapter four. Chapter five highlights the experimental setup used for understanding the chemical and structural properties of solid electrolytes. Chapter six contains the results derived from the experiments and gives a brief analysis of the results. A summary of the thesis work done and conclusions are presented in chapter seven. Finally the recommendations for future work are outlined in chapter eight.



## CHAPTER 2

### LITERATURE REVIEW

#### 2.1 California Institute of Technology

The Materials Science department at the California Institute of Technology developed a fuel cell made of a CsHSO<sub>4</sub> electrolyte membrane about 1.5mm thick operating at 150-160°C in a H<sub>2</sub>/O<sub>2</sub> configuration. At the transition temperature 50-150°C the conductivity of CsHSO<sub>4</sub> increases to a value of 10<sup>-3</sup> to 10<sup>-2</sup> Ω<sup>-1</sup>cm<sup>-1</sup>.

The solid acid electrolyte was prepared from an aqueous solution of Cs<sub>2</sub>CO<sub>3</sub> and H<sub>2</sub>SO<sub>4</sub>. A layer of the solid acid was sandwiched between two electrocatalysis layers comprised of CsHSO<sub>4</sub>, Pt black, carbon black and a volatile organic in a mass ratio of 6:10:1:1. These layers were then placed between two sheets of porous graphite current collectors. The entire assembly was uniaxially pressed at 490MPascal, to produce a dense electrolyte membrane of 1-1.5mm in thickness with good mechanical contact to the electrocatalyst layers.

The CsHSO<sub>4</sub> electrolyte used was a millimeter thick or thicker but for real applications micrometer thin films will be required to reduce the resistance of the electrolyte layer.[3]

## 2.2 The University of Texas at Austin

The Materials Science and Engineering department at the University of Texas at Austin studied the structural characterization and measured the superionic transitions of  $\text{CsHSO}_4$  before and after heating. The solid acid electrolyte was prepared as follows:  $\text{Cs}_2\text{SO}_4$  was first dissolved in a dilute sulfuric acid solution so that the molar ratio of  $\text{Cs}_2\text{SO}_4:\text{H}_2\text{SO}_4:\text{H}_2\text{O}$  is 1:2:12. After a complete dissolution of  $\text{Cs}_2\text{SO}_4$ , ethanol was added to the solution to precipitate  $\text{CsHSO}_4$ , which was then filtered, dried at 100 °C overnight, and stored in a vacuum desiccator before further characterization.

Structural characterization and the measurement of superionic transitions of  $\text{CsHSO}_4$  before and after heating were carried out, respectively, by X-ray powder diffraction and a Perkin-Elmer series 7 differential scanning calorimeter (DSC). The DSC experiments were carried out with approximately 10 mg of sample in a  $\text{N}_2$  atmosphere at a heating rate of 10 °C/min.[4]

In addition to the research being conducted at the California Institute of Technology and the University of Texas at Austin there has been considerable additional work done on solid acid compounds and a number of papers published explaining the mechanism of proton conductivity in solid acids by various methods, as well as the structure of different phases of the solid acid compound  $\text{CsHSO}_4$ . The mechanism of proton conductivity and the structure of different phases of  $\text{CsHSO}_4$ , as mentioned in the technical papers, are summarized below.

$\text{CsHSO}_4$  crystals undergo two phase transitions III-II at 100°C and II-I at 141°C. A hydrogenous  $\text{CsHSO}_4$  sample grown from an aqueous solution crystallizes in a monoclinic phase III. In phase III the crystals exhibit a high plasticity due to ferroelastic

twinning. The crystal structure consists of zigzag chains of hydrogen bonds linking  $\text{SO}_4$  tetrahedra. No phase transitions occur when this phase is cooled to liquid helium temperatures. When heated above  $100^\circ\text{C}$  phase III transforms into phase II which is also monoclinic. It differs from phase II in terms of lattice parameter, smaller unit cell volume and by the organization of hydrogen bonds. The distance between the nearest protons in different hydrogen bond chains is considerably larger in phase II than in phase III. At a temperature of  $141^\circ\text{C}$  phase II transforms into phase I which exhibits an extremely high protonic mobility resulting in high protonic conductivity. Phase I is tetragonal and contrary to the lower temperature phases, each  $\text{SO}_4$  can adopt not one but four crystallographically equivalent orientations. As a result, the number of possible proton positions in the unit cell becomes larger than the number of protons. The hydrogen bonded network becomes dynamically disordered allowing protons to move through the lattice by jumping to vacant positions. Proton jumps are associated with reorientations of  $\text{SO}_4$  tetrahedra. Since the transition is primarily driven by the disordering of  $\text{SO}_4$  tetrahedra and the proton disorder is a secondary effect the isotope effect on the transition temperature is absent.[5,6,7,8,9]

## CHAPTER 3

### THEORY OF SOLID ACIDS

#### 3.1 Structure

There are three important concepts necessary to describe the structure of solid acids:

- atomic bonding,
- coordination, and
- order-disorder.

Solid acids can be represented by the general chemical formula:  $M_aH_b(XO_4)_c$ , where M is a monovalent or divalent cation,  $XO_4$  is a tetrahedral oxy-anion, and a, b, c are integers. The structure of solid acids is comprised of hydrogen-bonded tetrahedral oxy-anions charge balanced by a host lattice of cations.

##### 3.1.1 Atomic Bonding

The theory of atomic bonding is a useful concept for the characterization and prediction of the structure of solids. Solids are held together by cohesive forces, which are the electrostatic interaction between the negative charges of electrons and the positive charges of the nuclei. The cohesive forces between atoms may be termed chemical or atomic bonds. Further, chemical bonds are classified as ionic or electrostatic bonds, covalent bonds, and metallic bonds.

The structure of solid acids is usually dominated by electrostatic or ionic bonding. When one or more electrons are transferred from one atom to another, they form a cation and an anion respectively. An ionic bond is formed when there is an electrostatic attraction between positively and negatively charged ions.[10,11,12,13]

### **3.1.2 Hydrogen Bonding**

A major contribution in the structure of solid acids is a fourth type of bond, known as the hydrogen bond. The hydrogen bond is defined as an atom of hydrogen attracted by strong forces to two atoms, instead of one, so as to act as a bond between them. [11]

While compared to other types of bonds, the hydrogen bond is to a certain extent weak, but it plays an important role in determining the structure and properties of solid acids. The attraction between hydrogen-bonded atoms is mostly due to large ionic forces since the hydrogen atom containing only a single 1s electron can form only one covalent bond. In the case of solid acids with hydrogen bonds between two oxygen atoms, the two oxygen atoms are labeled as the proton donor oxygen atom ( $O_d$ ), where the proton lies within the electron density of the oxygen atom and the bond most closely resembles a covalent bond, and the proton acceptor oxygen atom ( $O_a$ ), which is hydrogen-bonded to  $O_d$  via largely ionic forces.

For solid acid compounds, hydrogen bonds demonstrate unique hydrogen bond geometries within the hydrogen bonds namely, intra-hydrogen bonds, and inter-hydrogen bonds.[11,12,13]

### 3.1.2.1 Intra-Hydrogen Bonds

Hydrogen bonds between oxygen atoms can be categorized according to their strength, which is related to the donor oxygen to hydrogen distance ( $d_{O_d-H}$ ), and the donor to acceptor oxygen distance ( $d_{O_d...O_a}$ ). The strength of a hydrogen bond increases inversely with the covalency of the  $O_d-H$  bond, such that the hydrogen bond strength increases as the hydrogen bond character transitions from being largely ionic to mostly covalent.[11,12,13]

Table 3.1 Correlation Between Hydrogen Bond Types and Bond Character [12]

Bond Strength	$d_{O_d-H}(^{\circ}A)$	$d_{O_d...O_a}(^{\circ}A)$	Character
Strong	1.3 to 1.0	2.4 to 2.6	covalent
Medium	1.02 to 0.97	2.6 to 2.7	polar covalent
Weak	Below 1.1	2.7 to 3	ionic

Depending on the local symmetry of oxygen atoms participating in the hydrogen bond, the hydrogen bonds between oxygen atoms can be further classified into the following types.

If both oxygen atoms participating in a hydrogen bond occupy crystallographically equivalent positions, then the bond is symmetric, whereas, if the oxygen atoms occupy crystallographic distinct positions then the bond is asymmetric.

Table 3.2 is a schematic representation of the hydrogen bond potential energies  $E(r)$  (or potentials) as a function of interatomic distance between two oxygen atoms for strong, medium, and weak symmetric and asymmetric bonds.

For symmetric and asymmetric strong hydrogen bonds, at hydrogen bond distances less than  $2.4 \text{ }^{\circ}A$ , there is no distinction between the donor and acceptor oxygen

atoms and the hydrogen atom sits equidistant between the oxygen atoms in single-well potential.

Table 3.2 Effects of Symmetry on Strong, Medium and Weak Hydrogen Bonds [12]

Bond Type	Symmetric	Asymmetric
Strong		
Medium		
Weak	Not generally observed	

At medium bond strengths, with a hydrogen bond distance of  $\sim 2.6$  Å, for symmetric and asymmetric bonds the hydrogen atom can reside near either oxygen atom, in one minimum of a double-well potential. At sufficiently high temperatures, thermal

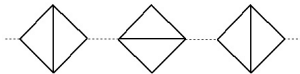
oscillations can allow the hydrogen atom to overcome the potential barrier between the minima in the double-well potential, partially occupying each position—this is known as hydrogen bond disorder. In table 3.2, for medium strength asymmetric hydrogen bonds both single-well potentials, case (1), which are not disordered and double-well potentials, case (2), which are disordered, are possible.

At hydrogen bond distances greater than 2.9 Å (weak hydrogen bonds), symmetric bonds are not generally observed and for asymmetric bonds the hydrogen atom lies within the minimum of a single-well potential, close to the donor oxygen atom.

### 3.1.2.2 Inter-Hydrogen Bonds

Further than intra-hydrogen bond geometry, the structure of solid acid compounds can also exhibit a wide variety of inter-hydrogen bond geometries, or networks. In general, the distribution of hydrogen bonds can exhibit zero, one, two, and three-dimensional networks depending on the density of hydrogen bonds. The type of hydrogen bond network depends on the ratio of hydrogen to tetrahedral oxy-anions (H/XO<sub>4</sub>). The CsHSO<sub>4</sub> solid acid has one hydrogen atom per XO<sub>4</sub> and tends to exhibit one-dimensional network in the form of chains.[11]

Table 3.3 Inter-Hydrogen Bond Networks Exhibited by CsHSO<sub>4</sub> Solid Acid [13]

Dimensionality	Networks	H/XO <sub>4</sub>	Example
1-D	<p style="text-align: center;">Chains</p> 	1	CsHSO <sub>4</sub>



### 3.2 Coordination

The coordination of an atom is defined by the number of surrounding nearest neighbor atoms. Coordination plays an important role in the arrangement of atoms in solids, and is influenced principally by the type of bonding and the relative size of atoms (or ions) in a solid. From simple geometric considerations and assuming a rigid sphere model for ions, the structure of ionic solids can often be inferred from the relative sizes of the constitutive ions.[13]

### 3.3 Order–Disorder

Order–disorder in solid acid structures is an important feature in identifying the properties of these compounds. The two main types of order–disorder phenomena observed in solid acids which describe the arrangement of atoms are

- structural disorder, in which a single atomic species partially occupies multiple crystallographic positions; and
- chemical disorder, in which multiple atomic species occupy the same crystallographic position.

Structural disorder can be broken into two general categories:

- Static disorder, when a single atomic species is randomly distributed over multiple crystallographic positions.
- Dynamic disorder, resulting from thermally activated atomic species moving between two or more crystallographic positions.

Of the above mentioned categories dynamic disorder is an important concept in understanding the properties of solid acid compounds.[11,12,13]

### **3.3.1 Dynamic Disorder**

Dynamic disorder is responsible for ferroelectric and superprotonic conductivity properties exhibited by solid acid compounds. The dynamic disorders exhibited in solid acids are as follows:

- Intra-hydrogen bond disorder,
- Inter-hydrogen bond disorder, and
- Oxy-anion disorder.

The first of these is responsible for ferroelectric transitions in solid acids, and the second and third, being closely related to each another, are responsible for superprotonic behavior.

### **3.3.2 Intra-Hydrogen Bond Disorder**

Intra-hydrogen bond disorder occurs in medium strength symmetric and asymmetric hydrogen bonds, in which there are two crystallographic positions separated by a potential barrier for a single hydrogen atom. At low temperatures there is insufficient thermal energy for the hydrogen atom to overcome the potential barrier, and the structure becomes ordered with respect to the intra-hydrogen bond—the hydrogen atom resides in just one crystallographic position. Upon heating, thermal oscillations of the hydrogen atom become sufficient to overcome the potential barrier between the two crystallographic positions and the crystallographic structure becomes disordered with respect to the intra-hydrogen bond. In terms of properties, this transition from order to disorder in solid acids leads to a ferroelectric to paraelectric transition. [11, 13]

### **3.3.3 Inter-Hydrogen Bond Disorder**

Upon heating some solid acids, the oxy-anions are set free between crystallographically equivalent positions, while simultaneously breaking and reforming new hydrogen bonds—a superprotonic phase transition. The hydrogen bond is thus distributed among several crystallographic positions, i.e., the inter-hydrogen bonding becomes disordered. [11, 13]

### **3.3.4 Oxy-Anion Disorder**

Dynamic structural oxy-anion disorder occurs when the oxygen atoms of structural tetrahedral oxy-anions partially occupy crystallographically equivalent positions. Due to the strong bonding between the oxygen atoms and the central tetrahedral atom, the overall tetrahedral structure is maintained, leading to the release of the tetrahedron between these crystallographically equivalent positions, and manifesting in several possible orientations of the tetrahedron. [11, 13]

## **3.4 Properties**

Electrolytes in general possess high ionic conductivity and little or no electronic conductivity. Therefore, the ionic conductivity and specifically protonic conductivity, is the principle material property of solid acids investigated here. CsHSO<sub>4</sub> solid acid exhibiting high proton or superprotonic conductivity is of particular interest.

### **3.4.1 Ionic Conductivity**

A review of the basic underlying principles of ionic conduction is given here. Consider an isotropic solid where the material property conductivity  $\sigma$  is a scalar quantity that relates the current density  $I$  to an applied electric field  $E$  according to Ohm's law

$$I = \sigma E \quad (3.1)$$

In an electrolyte with only one type of charge carrier, the current density  $I$  for a concentration of charged carriers  $n$  each with charge  $q$  traveling with an average velocity of  $v$  is

$$I = nqv \quad (3.2)$$

The charge carrier mobility  $T$  is defined as

$$T = \frac{v}{E} \quad (3.3)$$

can be used to express the conductivity as

$$\sigma = nqT \quad (3.4)$$

When the concentration of particles  $n$  and the electric field  $E$  vary along the  $x$ -direction, the subsequent flux  $J$  (or number of charged carriers passing through an area per time) of charge carriers is equal to the product of the mean force on the particles  $F$ ,  $n$  number of particles per unit volume, charge  $q$ , and their mobility per charge  $T/q$

$$J = -\frac{nT}{q} F = -\frac{nT}{q} \left( \frac{\partial \mu}{\partial x} + qE \right) \quad (3.5)$$

where  $\mu$  ( $= \partial G / \partial n$ ) is the chemical potential of the charge carriers. In the absence of an electric field ( $E = 0$ ) this reduces to

$$J = -\frac{nT}{q} \left( \frac{\partial \mu}{\partial x} + qE \right) \quad (3.6)$$

The flux of particles can also be expressed in terms of a charge carrier diffusion coefficient  $D$  according Fick's first law

$$J = -D \frac{\partial n}{\partial x} \quad (3.7)$$

Then, from the definition of chemical potential in dilute solutions

$$\mu = \mu_0 + k_B T \ln n \quad (3.8)$$

where  $k_B$  is the Boltzmann constant, and  $T$  is temperature, and differentiating with respect to  $x$

$$\frac{\partial \mu}{\partial x} = \frac{k_B T}{n} \left( \frac{\partial n}{\partial x} \right) \quad (3.9)$$

Now equating Equations 3.6 and 3.7, and using the previous relationship the diffusion coefficient can be related to the mobility of the charge carriers according to the Nernst-Einstein equation,

$$u = \frac{qD}{k_B T} \quad (3.10)$$

and substituting this into Equation 3.4 gives

$$\sigma = \frac{nq^2 D}{k_B T} \quad (3.11)$$

Assuming uncorrelated motion of the charge carrying species a random walk model can be adopted to describe the diffusion coefficient, such that

$$D = \gamma a_0^2 \omega \quad (3.12)$$

where  $\gamma$  is a geometric factor depending on the structure of the solid,  $a_0$  is the distance the mobile charge carrier “jumps” between vacant crystallographic sites, and  $\omega$  is the frequency at which the charge carrier jumps. The jumping of charge carriers between crystallographic sites is a thermally activated process, which is best described by an Arrhenius-type temperature dependence,

$$\omega = \omega_0 \exp \left( - \frac{\Delta G_a}{k_B T} \right) \quad (3.13)$$

where  $\omega_0$  is the attempt frequency and  $\Delta G_a$  is the Gibbs free energy for activation of this process. This leads to a diffusion coefficient that varies with an Arrhenius behavior,

$$D = \gamma a_0^2 \omega_0 \exp\left(\frac{\Delta G_a}{k_B T}\right) \quad (3.14)$$

$$= D_0 \exp\left(\frac{\Delta G_a}{k_B T}\right) \quad (3.15)$$

where the pre-exponential factor  $D_0 = \gamma a_0^2 \omega_0$ . The Gibbs free energy of activation can be expressed in terms of an activation entropy  $\Delta S_a$  and enthalpy  $\Delta H_a$

$$\Delta G_a = \Delta H_a - T\Delta S_a \quad (3.16)$$

Similarly, the activation enthalpy can be expressed in terms of an activation energy  $\Delta E_a$  and volume  $\Delta V_a$

$$\Delta H_a = \Delta E_a + P\Delta V_a \quad (3.17)$$

where the activation volume is often neglected at ambient pressures. Using these thermodynamic relationships and combining Equations 3.4, 3.10, and 3.14 the Arrhenius relationship for the conductivity of a solid can be written as

$$\sigma T = A_0 \exp\left(-\frac{\Delta H_a}{k_B T}\right) = A_0 \exp\left(-\Delta E_a - \frac{P\Delta V_a}{k_B T}\right) \quad (3.18)$$

where the pre-exponential factor  $A_0$  is

$$A_0 = \frac{D_0 n q^2}{k_B} \exp\left(\frac{\Delta S_a}{k_B}\right) \quad (3.19)$$

$$= \frac{\gamma a_0^2 \omega_0 n q^2}{k_B} \exp\left(\frac{\Delta S_a}{k_B}\right) \quad (3.20)$$

Thus, we have derived an expression for the ionic conductivity of an isotropic solid in terms of intrinsic material properties as a function of temperature that closely models the bulk behavior of real ionic solids.[14,15]

### 3.4.2 Protonic Conductivity

There are five basic mechanisms for proton motion in solids:

- atomic diffusion,
- proton-displacement,
- molecular reorientation,
- vehicle mechanism, and
- Grotthus mechanism.

#### 3.4.2.1 Atomic Diffusion

This type of proton motion is simply coupled proton-electron diffusion, which is common in materials such as metal hydrides, like  $\text{Li}_3\text{AlH}_6$  and  $\text{Na}_3\text{AlH}_6$ . In such materials, the hydrogen can donate its electron density to the host matrix, accept electron density, or simply remain neutral.[12,13]

#### 3.4.2.2 Proton Displacement

This proton motion occurs when a proton “hops” along a hydrogen bond from one minima of a double-well potential to the other. This type of proton motion is quite common in solid acid compounds, and is responsible for ferroelectric behavior in solid acids, such as  $\text{KH}_2\text{PO}_4$ . [12,13]

#### 3.4.2.3 Molecular Reorientation

Also referred to as dipole reorientation, in this process a proton rides “piggy-back” a molecule undergoing a reorientation, rotation, or tumble. This motion was first proposed to describe proton transport in ice, but is also commonly observed in solid acid compounds, as well as liquid acids. [12,13]

#### **3.4.2.4 Vehicle Mechanism**

In this mechanism, proton translation is associated with the diffusion of polyatomic species. In this type of proton motion, a proton rides “piggy-back” on a mobile molecule, which may carry a positive charge (e.g.  $\text{NH}^{+4}$ ,  $\text{OH}^{+3}$ ,  $\text{O}_2\text{H}^{+5}$ ,  $\text{O}_3\text{H}^{+7}$ ), a negative charge (e.g.  $\text{NH}^{-2}$ ,  $\text{OH}^-$ ), or be neutral (e.g.  $\text{NH}_3$ ,  $\text{H}_2\text{O}$ ). The vehicle mechanism is, perhaps, the most common type of proton transport mechanism, and is exhibited by many fast-proton conductors, such as Nafion, in which  $\text{H}_3\text{O}^+$  ions are transported along sulfonic acid functional groups ( $\text{SO}_3^-$ ), within a polymer host matrix.[12,13]

#### **3.4.2.5 Grotthus Mechanism**

This mechanism is a cooperative process involving both a molecular (dipole) reorientation and proton-displacement. Superprotonic solid acids, such as  $\text{CsHSO}_4$ , conduct protons via this process. In these superprotonic solid acids, the oxyanion rearranges between crystallographically equivalent positions while carrying a proton with it, then the proton “hops” along a hydrogen bond to another oxyanion, followed by another oxyanion reorientation, and so on.[12,13]

### **3.5 Phase Transitions**

Phase transitions are of fundamental importance to this work since the superprotonic behavior in solid acid compounds is associated with a structural phase transition. Here, a general description of phase transitions will be given, as well as a specific description of superprotonic phase transitions.



### 3.5.1 General Characterization

A phase is a homogeneous solution of matter bounded by a surface so that it is mechanically separated from any other portion. A phase transition is a transformation of matter induced by a change in a thermodynamic function, such as temperature  $T$ , pressure  $P$ , volume  $V$ , or entropy  $S$ , from one phase to another phase that is noticeable from the first. For the purpose of this work phase transitions are identified by a discontinuous change in the extensive thermodynamic variables of a substance, such as volume  $V$ , entropy  $S$ , magnetization  $M$ , polarization  $P$ , while varying an intensive variable, such as pressure  $P$ , temperature  $T$ , magnetic field  $B$ , or electric field  $E$ . Specifically, for transitions in which there is a discontinuous change in the entropy through the phase transition while varying the temperature, there will also be a change in enthalpy  $\Delta H$  or latent heat  $Q$  associated with the transition. This sort of phase transition is known as a first order phase transition. If the entropy is continuous, but its first derivative with respect to temperature, or heat capacity  $C_p$  is discontinuous, then the phase transition is said to be of second order, and if the entropy and heat capacity are continuous, and the derivative of the heat capacity  $\partial C_p / \partial T$  is discontinuous, the transition is third order, and so on.[13]

$$C_p = T \left( \frac{\partial S}{\partial T} \right)_p \quad (3.21)$$

In this work, first order solid–solid phase transitions are of key interest. For these transitions the change in extensive thermodynamic variables such as  $V$  and  $M$  are negligible compared to the change in  $S$ .

$$T = \frac{\partial E}{\partial S} \quad (3.22)$$

### 3.5.2 High Temperature Proton Conduction in Solid Acids

At higher temperatures a highly disordered state leads to fast local dynamics of the anion tetrahedra and subsequent proton transition via the Grothhuss mechanism. The physical reorientations of the tetrahedra in these phases suggest that the tetrahedra are rearranging much faster than the protons being transferred. Due to an increase in symmetry across the phase transition there is a disorder on the oxygen sites, which causes the tetrahedra to rotate freely between crystallographically identical positions. This nearly free rotation of the tetrahedra creates more crystallographically equivalent proton sites than the protons, resulting in a “dynamically” disordered hydrogen-bonded network. The combination of fast tetrahedral dynamics and proton transitions along hydrogen bonds of a disordered network results in high protonic conductivity.

The room temperature phase of CsHSO<sub>4</sub>-II is monoclinic, made up of zigzag chains of hydrogen bonded SO<sub>4</sub> tetrahedra alternating with zigzag rows of cesium atoms. There are four crystallographically distinct oxygens, two of which are involved in asymmetric hydrogen bonds. After going into the superprotonic tetragonal phase the oxygens become crystallographically identical and all oxygens participate in hydrogen bonds. There are two possible orientations of the tetrahedra, resulting in  $\frac{1}{2}$  and  $\frac{1}{4}$  occupancy of the oxygen and proton sites, respectively whereby the hydrogen bonds connect the oxygens. The method of proton conduction can be summarized as rapid reorientations of the SO<sub>4</sub> group forming a dynamically disordered network of hydrogen bonds through which protons can jump from one tetrahedron to the next. This mechanism of proton transport is responsible for the high conductivity in all superprotonic phases of solid acids. [12, 13]

## CHAPTER 4

### DESIGN AND DEVELOPMENT OF SOLID ACID ELECTROLYTE

Two procedures were pursued to prepare CsHSO<sub>4</sub> :

- Reaction of Cs<sub>2</sub>SO<sub>4</sub> and H<sub>2</sub>SO<sub>4</sub> such that the ratio of Cs<sub>2</sub>SO<sub>4</sub> to H<sub>2</sub>SO<sub>4</sub> is 1:1 and,
- Reaction of Cs<sub>2</sub>CO<sub>3</sub> and H<sub>2</sub>SO<sub>4</sub> such that the ratio of Cs<sub>2</sub>CO<sub>3</sub> to H<sub>2</sub>SO<sub>4</sub> is 1:2

#### 4.1 CsHSO<sub>4</sub> Prepared from Equimolar Amounts of Cs<sub>2</sub>SO<sub>4</sub> and H<sub>2</sub>SO<sub>4</sub>

##### *Sulfuric Acid*

Molecular Weight = 98.08

Normality = 36

Specific Gravity = 1.84 gm/ml

Concentration = 98.8 %

##### *Cesium Sulfate*

Molecular Weight = 361.88

Equimolar amounts of cesium sulfate and sulfuric acid are required

For every 361.88 gm of Cs<sub>2</sub>SO<sub>4</sub> we need 98.08 gm of H<sub>2</sub>SO<sub>4</sub>

Pure H<sub>2</sub>SO<sub>4</sub> = 0.958 x 1.84

$$= 1.76272 \text{ gm/ml}$$

For each ml of H<sub>2</sub>SO<sub>4</sub>, the amount of Cs<sub>2</sub>SO<sub>4</sub> required =  $1.76272 \times \frac{361.88}{98.08}$

$$= 6.5038 \text{ gm}$$

The following procedure was employed to prepare CsHSO<sub>4</sub> : [19]

- First of all, equimolar amounts of Cesium Sulfate and concentrated sulfuric acid are dissolved in a small amount of DI water.
- The resulting solution is then concentrated under a flow of warm air in an oven at a temperature of 60°C until less than half the water has evaporated.
- Once half the water has evaporated, the solution is then cooled in a chiller at a temperature of 5°C.
- The precipitated crystalline solid is separated by filtration and then dried in a vacuum desiccator.
- The powdered sample is then dried in an oven at about 105°C to ensure that it is completely dry.
- The sample is then placed in a punch, base and die assembly for pressing in order to prepare pellets of 0.5” and 2.0”.

#### **4.2 CsHSO<sub>4</sub> Prepared from Cs<sub>2</sub>CO<sub>3</sub> and H<sub>2</sub>SO<sub>4</sub> such that Cs<sub>2</sub>CO<sub>3</sub>: H<sub>2</sub>SO<sub>4</sub> :: 1:2**

The amount of CsHSO<sub>4</sub> required to prepare 0.5” diameter and 1 mm thick pellet was calculated as follows:

*Sulfuric Acid*

Molecular Weight = 98.08

Normality = 36

Specific Gravity = 1.84 gm/ml

Concentration = 98.8 %

*Cesium Carbonate*

Molecular Weight = 325.82

The ratio of Cs<sub>2</sub>CO<sub>3</sub> to H<sub>2</sub>SO<sub>4</sub> is 1:2

For every 325.82 gm of Cs<sub>2</sub>CO<sub>3</sub> we need 98.08 x 2 = 196.16 gm of H<sub>2</sub>SO<sub>4</sub>

Pure H<sub>2</sub>SO<sub>4</sub> = 0.958 x 1.84

$$= 1.76272 \text{ gm/ml}$$

For each mil of H<sub>2</sub>SO<sub>4</sub>, the amount of Cs<sub>2</sub>CO<sub>3</sub> required =  $1.76272 \times \frac{325.82}{196.16}$

$$= 2.9278 \text{ gm}$$

The procedure adopted for preparing CsHSO<sub>4</sub> from Cs<sub>2</sub>CO<sub>3</sub> and H<sub>2</sub>SO<sub>4</sub> is same as that from Cs<sub>2</sub>SO<sub>4</sub> except that instead of Cs<sub>2</sub>SO<sub>4</sub>, Cs<sub>2</sub>CO<sub>3</sub> is to be used.

**4.3 Pellet Preparation**

The amount of CsHSO<sub>4</sub> required to prepare 0.5” and 2.0” diameter pellets with 1 mm thickness was calculated as follows:

**4.3.1 For 0.5” Diameter Pellet and 1 mm Thickness**

$$A = \frac{\pi d^2}{4}$$

$$A = \frac{\pi \times 0.5^2}{4}$$

$$A = 0.1963 \text{ inch}^2$$

Volume = A x thickness of the pellet

$$= 0.1963 \times 2.5^2 \times 0.1$$

$$\text{Volume} = 0.1226 \text{ cm}^3$$

Density of CsHSO<sub>4</sub> = 3.352 gm/cc

$$\text{Density} = \frac{\text{mass}}{\text{Volume}}$$

$$3.352 = \frac{\text{mass}}{0.1226}$$

$$\text{Mass} = 0.4109 \text{ gm of CsHSO}_4$$

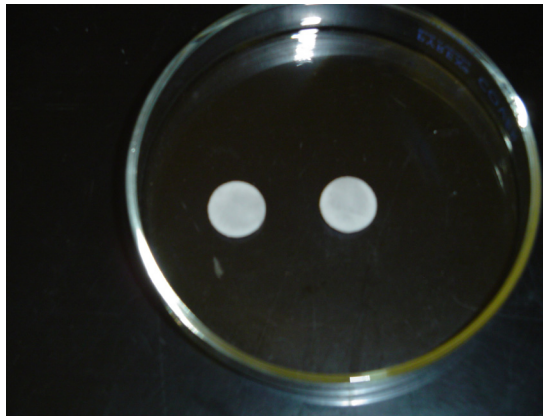


Fig 4.1 0.5" Diameter Pellets of CsHSO<sub>4</sub>

#### 4.3.2 For 2.0" Diameter Pellet and 1 mm Thickness

$$A = \frac{\pi d^2}{4}$$

$$A = \frac{\pi \times 2.0^2}{4}$$

$$A = 3.1415 \text{ inch}^2$$

$$\text{Volume} = A \times \text{thickness of the pellet}$$

$$= 3.1415 \times 2.5^2 \times 0.1$$

$$\text{Volume} = 1.9634 \text{ cm}^3$$

$$\text{Density of CsHSO}_4 = 3.352 \text{ gm/cc}$$

$$\text{Density} = \frac{\text{mass}}{\text{Volume}}$$

$$3.352 = \frac{\text{mass}}{1.9634}$$

Mass = 6.5813 gm of CsHSO<sub>4</sub>

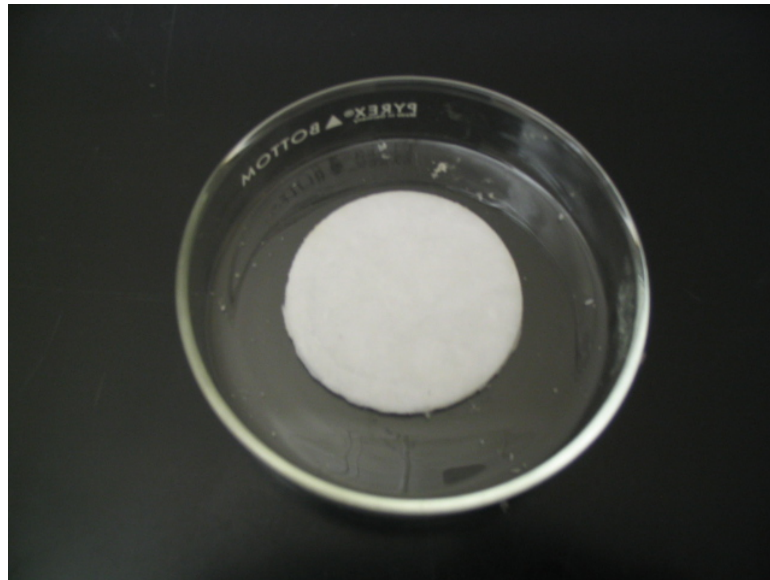


Fig 4.2 2” Diameter Pellet of CsHSO<sub>4</sub>

From literature [3] search it was observed that for 0.5” diameter disc with 1 mm thickness the amount of pressure required to press is 490MPascal. Table 4.1 indicates the amount of force required to press discs of different diameters.

Table 4.1 Amount of Force Required to Press Discs of Different Diameters

Disc Diameter (inches)	Press (tons)
0.6	12
0.8	17
2.0	110
3.5	350

#### 4.4 Die Design

The specifications of the die, punch and base for preparing 0.5” and 2.0” diameter pellets are as shown in table 4.2.

Table 4.2 Specifications of Die, Punch and Base

	Material	Hardness
Die	A2 Steel	40-50 Rockwell
Punch	A2 Steel	40-50 Rockwell
Base	A2 Steel	40-50 Rockwell

#### 4.4.1 Pellets of 0.5” Diameter

The design of the punch, die and base for preparing 0.5” diameter pellets is as shown in the figure 4.3.

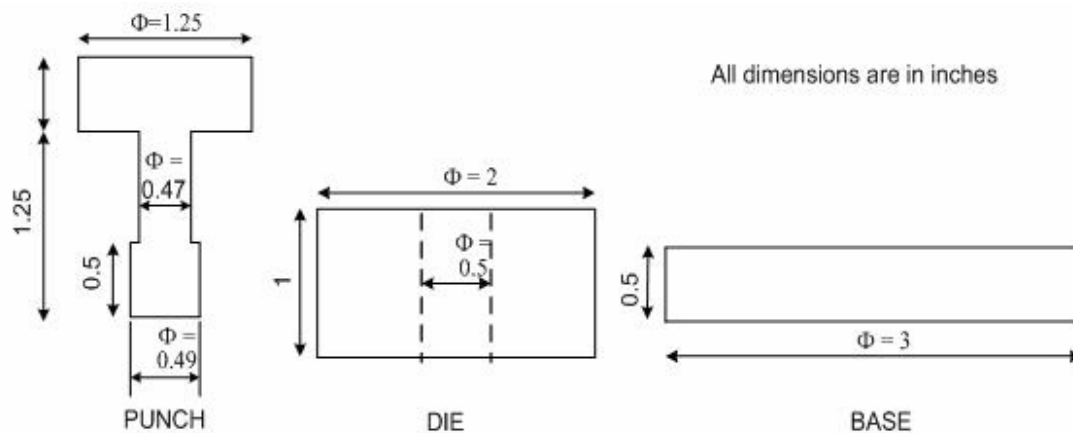


Fig 4.3 Design of Punch, Die and Base for Preparing 0.5” Diameter Pellets



The fabricated punch, die and base for preparing 0.5” diameter pellets is shown in figure 4.4



Fig 4.4 Fabricated Punch, Die and Base for Preparing 0.5” Diameter Pellets

The hydraulic press used for preparing 0.5” diameter pellets is as shown in figure 4.5.

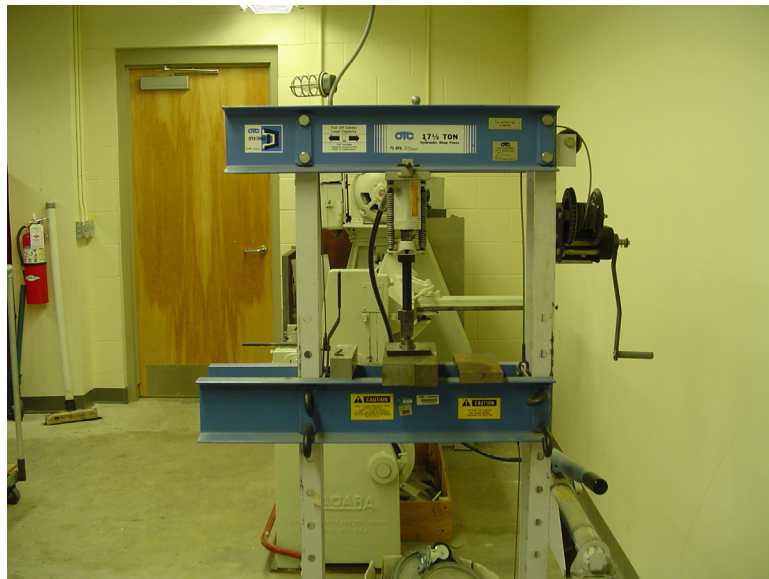


Fig 4.5 Hydraulic Press Used for Preparing 0.5” Diameter Pellets

#### 4.4.2 Pellets of 2.0" Diameter

The design of the punch, die and base for preparing 2.0" diameter pellets is as shown in the figure 4.6.

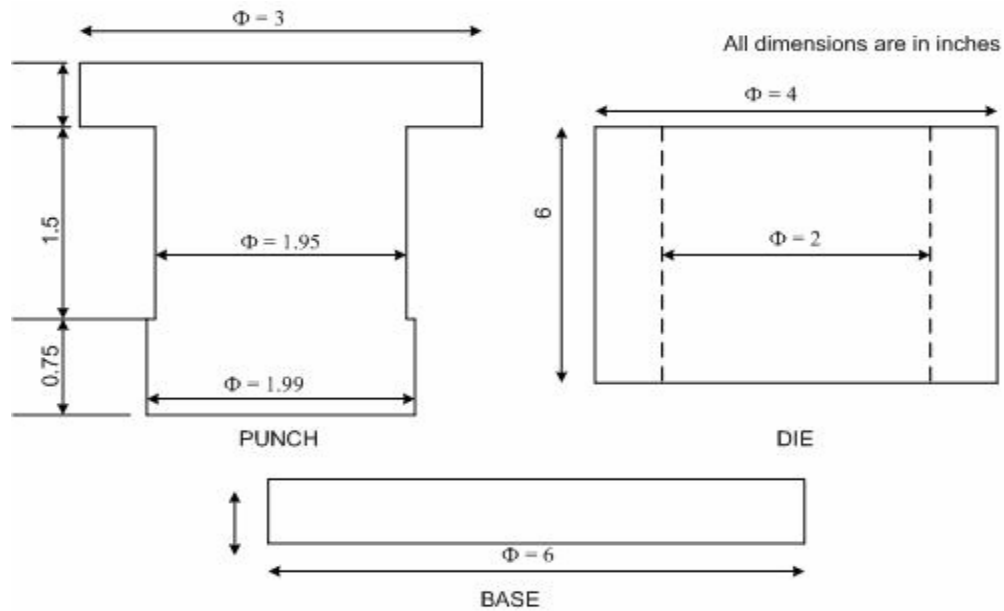


Fig 4.6 Design of Punch, Die and Base for Preparing 2.0" Diameter Pellets

The fabricated die, punch and base for preparing 2.0" diameter pellets is shown below.

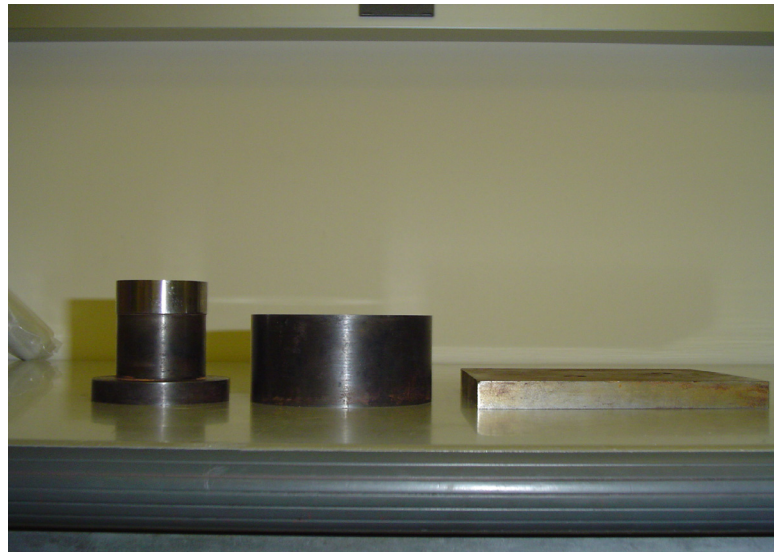


Fig 4.7 Fabricated Punch, Die and Base for Preparing 2.0" Diameter Pellets

The press used for preparing 2.0” diameter pellets is as shown in figure 4.8.



Fig 4.8 MTS Press Used for Preparing 2.0” Diameter Pellet

## CHAPTER 5

### THEORY OF EXPERIMENTAL MEASUREMENTS

#### 5.1 Impedance Measurement Theory

Protonic conductivity is the principle property of interest in the CsHSO<sub>4</sub> electrolyte. For this, extensive use of alternating current (AC) impedance spectroscopy has been made to characterize the protonic conductivity of this solid acid compound as a function of temperature at ambient pressure.

The advantage of an AC method is that there is no net movement of ions, thereby eliminating the need for an ion source. This method is implemented by placing an ionic conducting material under an alternating electric field  $E$ , with an angular frequency of  $\omega$  and amplitude  $E_0$ , which can be described by the complex time ( $t$ ) dependent wave function

$$E(t) = E_0 e^{j\omega t} \quad (5.1)$$

The current response  $I(t)$  generated by this electric field in the material being tested, as shown in Figure 5.1, can be described by a similar time dependent wave function with some amplitude  $I_0$ , plus a phase shift  $\Phi$ ,

$$I(t) = I_0 e^{j(\omega t + \Phi)} \quad (5.2)$$

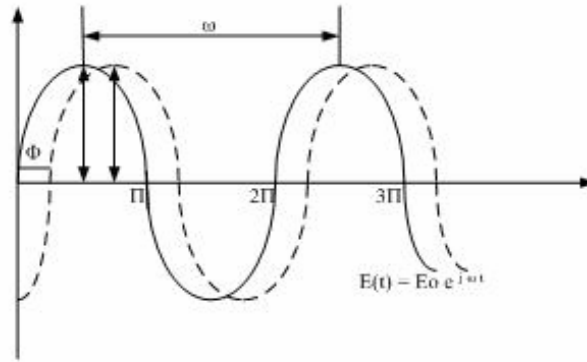


Fig 5.1 Time Dependent Wave Function

From Ohm's law,

$$E(t) = I(t) \cdot Z \quad (5.3)$$

where  $Z$  is the complex impedance characterized by a real component  $Z'$  and an imaginary component  $Z''$

$$Z = Z' + jZ'' \quad (5.4)$$

The reciprocal of impedance is admittance  $Y$  and is given as

$$Y = \frac{1}{Z} = Y' + jY'' \quad (5.5)$$

Rewriting Ohm's law using admittance

$$Y(\Phi) = \frac{I(t)}{E(t)} = \frac{I_0 e^{j(\omega t + \Phi)}}{E_0 e^{j\omega t}} = \frac{I_0}{E_0} (\cos\Phi + j\sin\Phi) \quad (5.6)$$

When a material's current response is at a frequency at which no phase shift occurs ( $\Phi = 0$ ), then equation becomes

$$Y(0) = \frac{I_0}{E_0} = \frac{1}{R} \quad (5.7)$$

where  $R$  is considered as the real resistance of the material under test. As the frequency  $\omega$  increases, the material's current response due to mobile charge carriers begins to lag

behind the applied electric field by some phase shift  $\Phi$ . This, in turn, leads to a capacitive response from the material under test. This capacitive response is at a maximum at some characteristic frequency  $\omega_0$ , when the current response is exactly  $90^\circ$  out of phase with the applied electric field, or when  $\Phi = \Pi/2$ . Capacitance  $C$ , defined in terms of applied electric field and charge  $q$ ,

$$C = \frac{q(t)}{E(t)} \quad (5.8)$$

can be used to evaluate the imaginary component of the admittance, by substituting in for  $q(t)$  into the definition of current,

$$I(t) = \frac{d}{dt} q(t) = C \frac{d}{dt} E(t) \quad (5.9)$$

Now, substituting in for  $E(t)$ , using equation 5.1, gives

$$I(t) = j\omega C E(t) \quad (5.10)$$

From Ohm's law, and the above result, the imaginary component of the admittance for  $\Phi = \Pi/2$  is

$$Y(\frac{\Pi}{2}) = \frac{I(t)}{E(t)} = 1 + j\omega C = j\omega C \quad (5.11)$$

With the real and imaginary components (at  $\Phi = 0$ , and  $\Pi/2$ , respectively) of the complex admittance the complete polar form can be written:

$$Y = Y' + jY'' = \frac{1}{R} + j\omega C \quad (5.12)$$

Similarly, with some rearranging the complex impedance can be written:

$$Z = \frac{1/R}{(1/R)^2 + (\omega C)^2} - \frac{j\omega C}{(1/R)^2 + (\omega C)^2} \quad (5.13)$$

It should be noted that a similar analysis could have been carried out using the impedance, rather than the admittance; however, the result is an expression in which the real component of the impedance increases with frequency, which is not logical.

In Figure 5.2, the complex impedance as a function of frequency  $\omega$  or “Nyquist” plot of the equation is presented. Here the apex is defined by a characteristic frequency  $\omega_0$  in terms of the resistive and capacitive response of the material under test,

$$\omega_0 = \frac{1}{RC} \quad (5.14)$$

and the diameter of the semi-circle is given by the real resistance of the material  $R$ . These results lead to an equivalent RC circuit shown in Figure 5.3, which is commonly employed in the analysis of AC impedance results.[12,13]

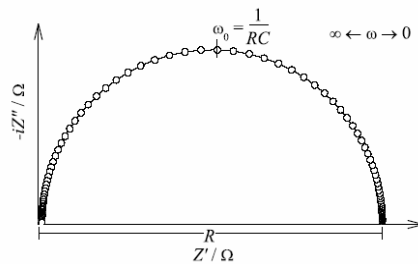


Fig 5.2 Nyquist Plot of the AC Impedance of a Material as a Function of Frequency  $\omega$ .

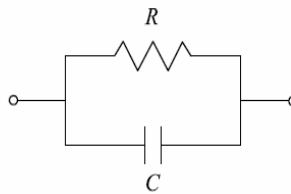


Fig 5.3 Equivalent RC Circuit

## 5.2 Differential Scanning Calorimetry (DSC)

Differential scanning calorimetry is a technique used to study the thermal transitions and heat flow of a chemical compound.

The compound weighs up to 15 mg and is heated in the apparatus as shown in figure 5.4

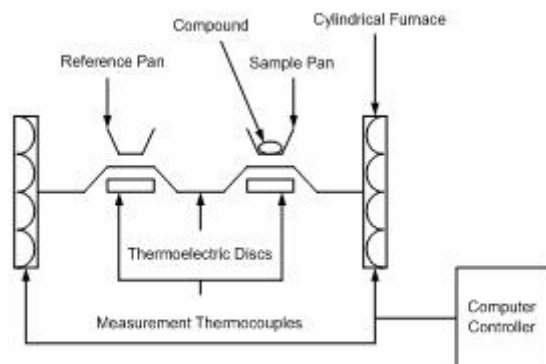


Fig 5.4 Differential Scanning Calorimetry Setup

In this DSC design, two pans sit on a pair of identically positioned platforms connected to a furnace by a common heat flow path. In one pan the sample is placed. The other one is the reference pan which is left empty. The DSC is interfaced with the computer used to control the furnace. The two pans are heated at a specific rate usually  $5/10^{\circ}\text{C}$  per minute. The software installed in the computer ensures consistent heating rate throughout the experiment and also that the two separate pans are heated at the same rate as each other.

A graph the temperature and the difference in heat flow between the sample and reference are plotted on the x and y axis respectively.

In a "heat flux" DSC, the sample material, encapsulated in a pan, and an empty reference pan sit on a thermoelectric disk surrounded by a furnace. As the temperature of the furnace is changed (usually by heating at a linear rate), heat is transferred to the



sample and reference through the thermoelectric disk. The differential heat flow to the sample and reference is measured by area thermocouples using the thermal equivalent of Ohm's Law.[22]

$$q = \frac{\Delta T}{R}$$

where  $q$  = sample heat flow

$\Delta T$  = temperature difference between sample and reference

$R$  = resistance of the thermoelectric disk

### **5.3 X-Ray diffraction**

X-Ray diffraction methods were exclusively used to identify the phases of the compounds. The diffraction measurements were performed on 0.5” diameter pellets at room temperature.

X-Ray diffraction is a versatile, non-destructive analytical technique for identification and quantitative determination of the various crystalline forms known as “phases” of compounds present in powdered and solid samples. Identification is achieved by comparing the x-ray diffraction pattern or diffractogram obtained from an unknown sample with an internally recognized database containing reference patterns for more than 70,000 phases. Modern computer controlled diffractometer systems use automatic routines to measure, record and interpret the unique diffractograms produced by individual constituents in even highly complex mixtures. X-ray diffraction of a sample provides information about the nature of phases present, the concentration levels of the phases present and the amorphous content of the sample.

## 5.4 Infrared Spectroscopy

The vibrational spectrum of  $\text{CsHSO}_4$  was measured in flowing nitrogen by infrared spectroscopy.

When a beam of electromagnetic radiation of intensity  $I_0$  is passed through a substance, it can either be absorbed or transmitted, depending upon its frequency,  $\nu$ , and the structure of the molecule it encounters. Electromagnetic radiation is energy and hence when a molecule absorbs radiation it gains energy as it undergoes a quantum transition from one energy state ( $E_{\text{initial}}$ ) to another ( $E_{\text{final}}$ ). The frequency of the absorbed radiation is related to the energy of the transition by Planck's law:  $E_{\text{final}} - E_{\text{initial}} = E = h\nu = hc/\lambda$ . Thus, if an allowed infrared transition exists which is related to the frequency of the incident radiation by Planck's constant, then the radiation can be absorbed. Conversely, if the frequency does not satisfy the Planck expression, then the radiation will be transmitted.

There are in general several types of motion that a molecule can possess namely translational, rotational and vibrational motion. Each of the vibrational motions of a molecule occurs with a certain frequency, which is characteristic of the molecule and of the particular vibration. The energy involved in a particular vibration is characterized by the frequency of the vibration, so that the higher the vibrational energy, the larger the frequency of the motion. According to the results of quantum mechanics, only certain vibrational energies are allowed to the molecule (the same may be said of rotational and translational energies), and thus only certain amplitudes are allowed. Associated with each of the vibrational motions of the molecule, there is a series of energy levels (or vibrational energy states). The molecule may be made to go from one energy level to a

higher one by absorption of a quantum of electromagnetic radiation, such that  $E_{\text{final}} - E_{\text{initial}} = h\nu$ . In undergoing such a transition, the molecule gains vibrational energy, and this is manifested in an increase in the amplitude of the vibration. The frequency of light required to cause a transition for a particular vibration is equal to the frequency of that vibration, so that we may measure the vibrational frequencies by measuring the frequencies of light which are absorbed by the molecule. Since vibrational motions in molecules often occur at frequencies of the order of about  $10^{14} \text{sec}^{-1}$ , then light of wavelength  $= c/\nu = 3 \times 10^{10} \text{ cm/sec}/10^{14} \text{sec}^{-1} = 3 \times 10^{-4} \text{ cm} = 3 \text{ microns}$  will be required to cause transitions. As it happens, light of this wavelength lies in the so-called infrared region of the spectrum. IR spectroscopy, then, deals with transitions between vibrational energy levels in molecules, and is therefore also called vibrational spectroscopy. An IR spectrum is generally displayed as a plot of the energy of the infrared radiation (expressed either in microns or wave numbers) versus the percent of light transmitted by the compound.[23]

## CHAPTER 6

### EXPERIMENTAL RESULTS

#### 6.1 Impedance Measurements Results

The conductivity of the potential electrolytes was measured by a.c. impedance spectroscopy using a 4294A Precision Impedance Analyzer. Conductivity measurements were taken on 0.5" diameter pellets which were obtained by uni-axially pressing the sample. Silver paint served as the electrode material. Measurements were made at a frequency of 1 MHz with an applied voltage of 0.5 V under ambient atmosphere.

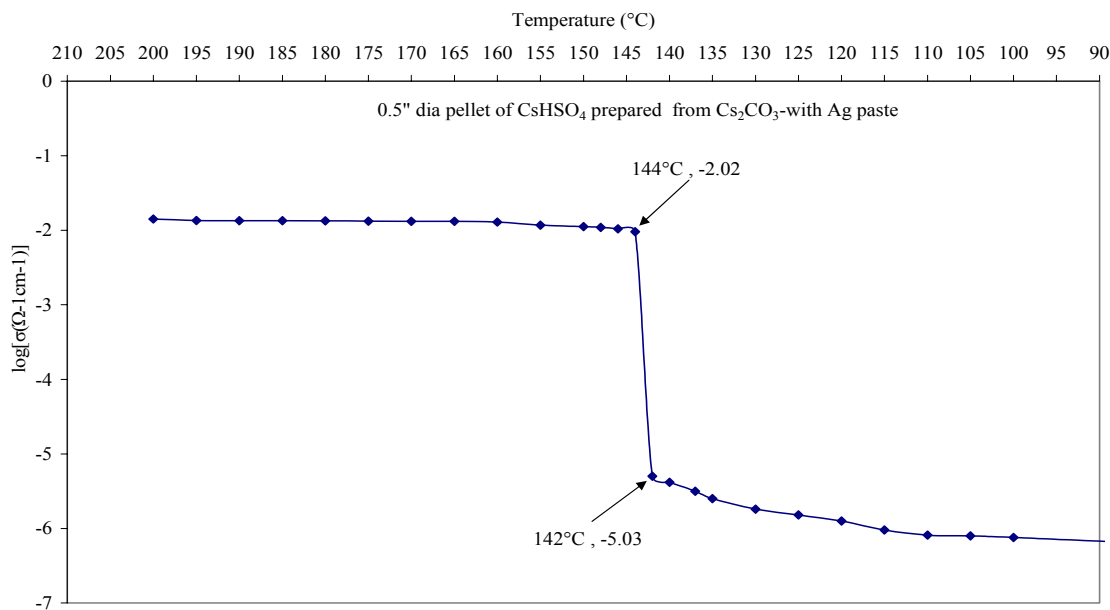


Fig 6.1 Log[conductivity] vs Temp for 0.5" Dia Pellet of CsHSO<sub>4</sub> from Cs<sub>2</sub>CO<sub>3</sub> with Ag Paste

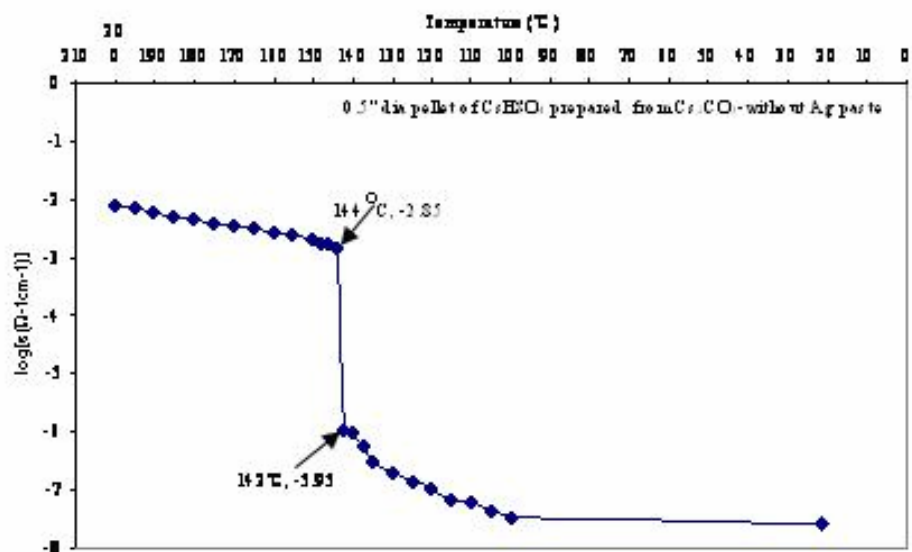


Fig 6.2 Log[conductivity] vs Temp for 0.5" Dia Pellet of CsHSO<sub>4</sub> from Cs<sub>2</sub>CO<sub>3</sub> without Ag Paste

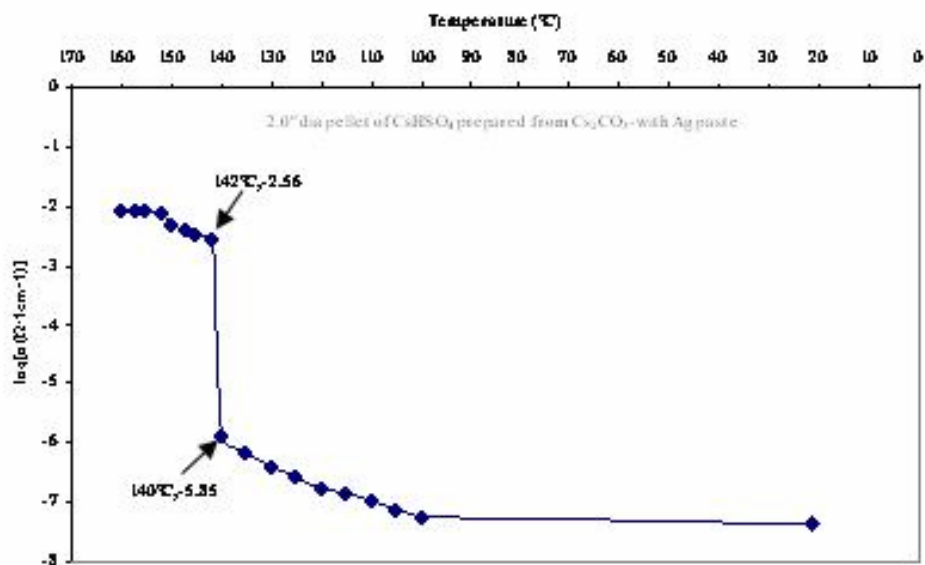


Fig 6.3 Log[conductivity] vs Temp for 2.0" Dia Pellet of CsHSO<sub>4</sub> from Cs<sub>2</sub>CO<sub>3</sub> with Ag Paste

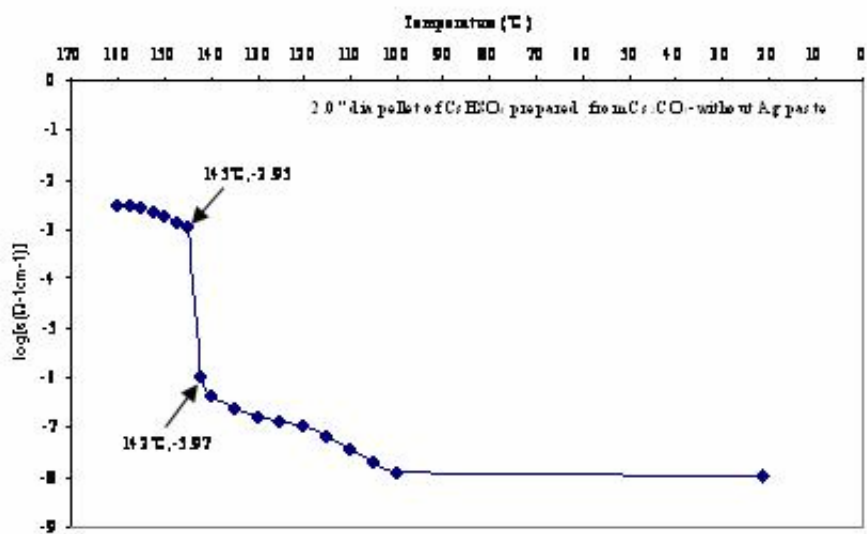


Fig 6.4 Log[conductivity] vs temperature for 2.0" diameter pellet of CsHSO<sub>4</sub> prepared from Cs<sub>2</sub>CO<sub>3</sub> without Ag paste

Fig 6.4 Log[conductivity] vs Temp for 2.0" Dia Pellet of CsHSO<sub>4</sub> from Cs<sub>2</sub>CO<sub>3</sub> without Ag Paste

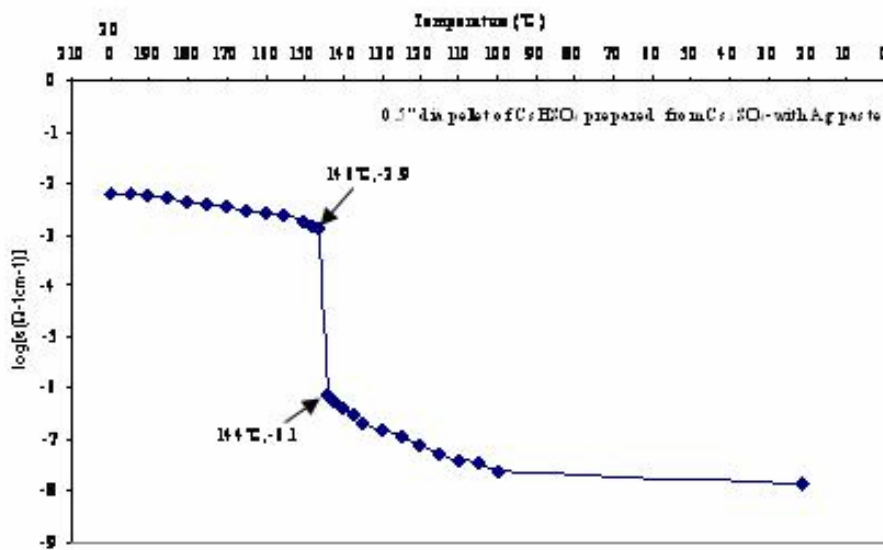


Fig 6.5 Log[conductivity] vs Temp for 0.5" Dia Pellet of CsHSO<sub>4</sub> from Cs<sub>2</sub>SO<sub>4</sub> with Ag Paste

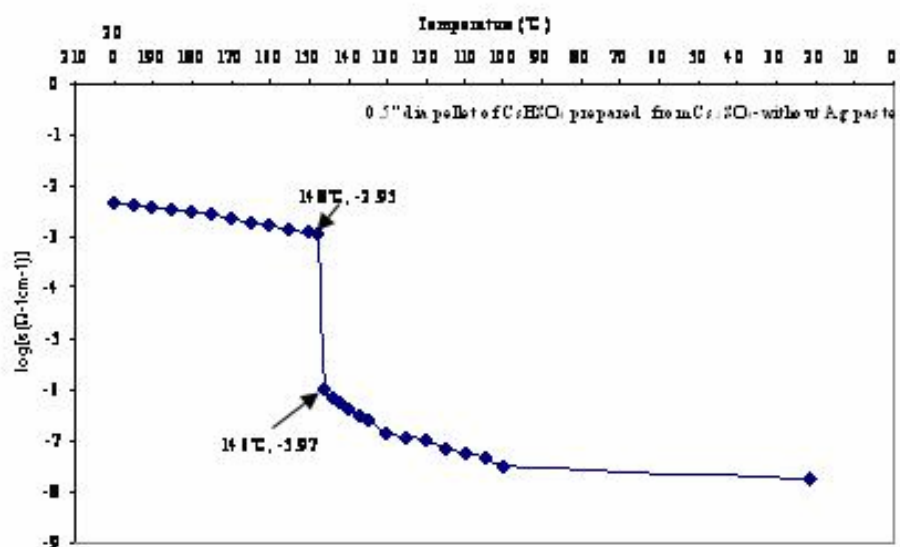


Fig 6.6 Log[conductivity] vs Temp for 0.5" Dia Pellet of CsHSO<sub>4</sub> from Cs<sub>2</sub>CO<sub>3</sub> without Ag Paste

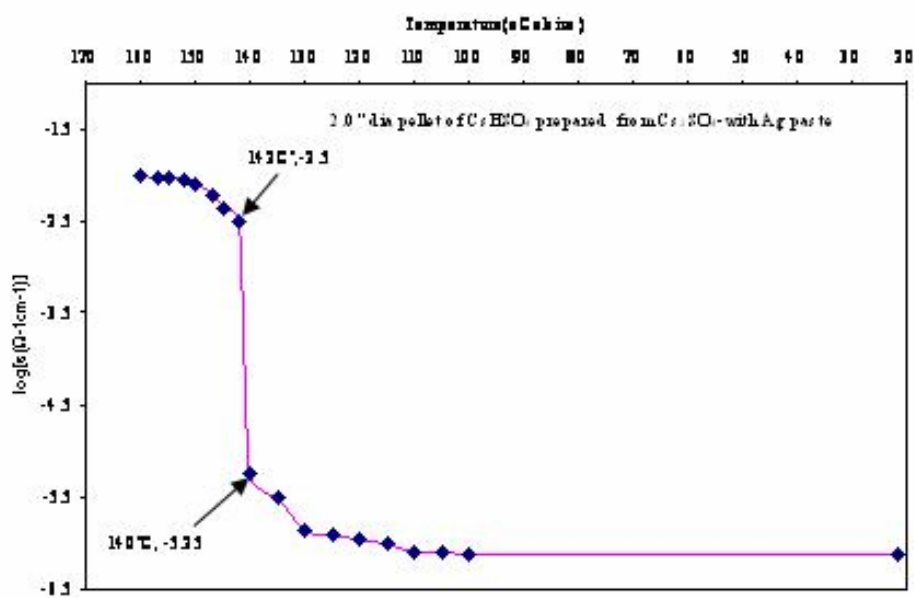


Fig 6.7 Log[conductivity] vs Temp for 2.0" Dia Pellet of CsHSO<sub>4</sub> from Cs<sub>2</sub>SO<sub>4</sub> with Ag Paste

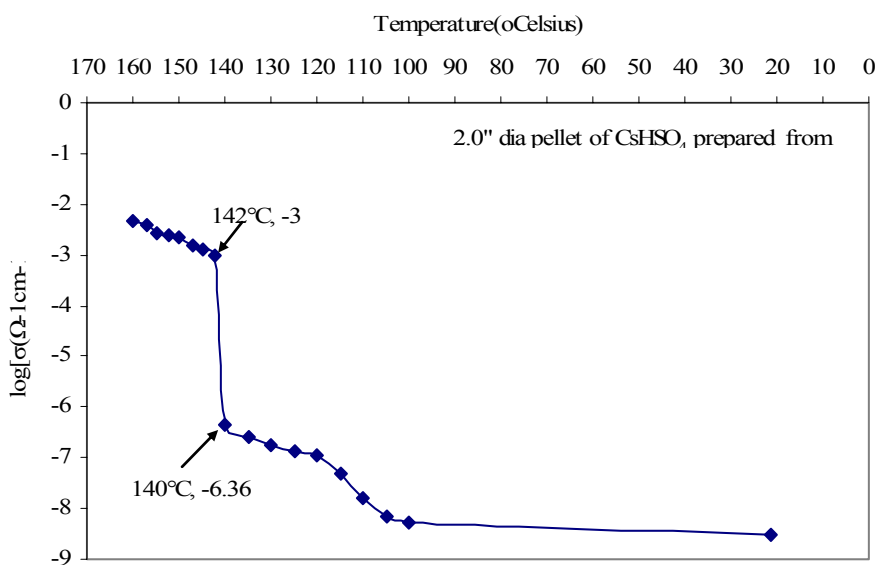


Fig 6.8 Log[conductivity] vs Temp for 2.0" Dia Pellet of CsHSO<sub>4</sub> from Cs<sub>2</sub>CO<sub>3</sub> without Ag Paste

Table 6.1 Impedance Measurements Results

		CsHSO <sub>4</sub> prepared from	Phase Transition Temperature	Log[σ(Ω <sup>-1</sup> cm <sup>-1</sup> )]
0.5" diameter pellet	With Ag paste	Cs <sub>2</sub> CO <sub>3</sub>	144°C	-2.02
	Without Ag paste	Cs <sub>2</sub> CO <sub>3</sub>	144°C	-2.85
2.0" diameter pellet	With Ag paste	Cs <sub>2</sub> CO <sub>3</sub>	142°C	-2.56
	Without Ag paste	Cs <sub>2</sub> CO <sub>3</sub>	145°C	-2.95
0.5" diameter pellet	With Ag paste	Cs <sub>2</sub> SO <sub>4</sub>	146°C	-2.9
	Without Ag paste	Cs <sub>2</sub> SO <sub>4</sub>	148°C	-2.95
2.0" diameter pellet	With Ag paste	Cs <sub>2</sub> SO <sub>4</sub>	142°C	-2.5
	Without Ag paste	Cs <sub>2</sub> SO <sub>4</sub>	142°C	-3



From the table 6.1 it can be concluded that  $\text{CsHSO}_4$  undergoes a superprotonic phase transition at a temperature of 140-150°C which is in agreement with the technical paper [3].

## 6.2 Differential Scanning Calorimetry (DSC) Results

The behavior of compounds with increasing temperature was investigated by differential scanning calorimetry. The presence and characterization of phase transitions above room temperature were accomplished by DSC measurements. The compound's response to heating and cooling was examined with a TA Instrument Q Series DSC in a flowing helium atmosphere. The heating and cooling rates were 10°C per minute.

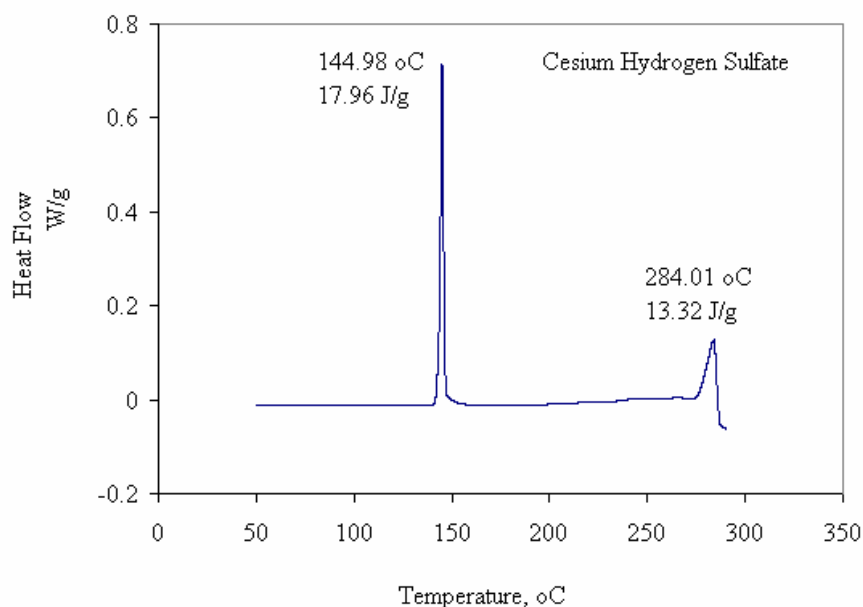


Fig 6.9 DSC Plot of  $\text{CsHSO}_4$

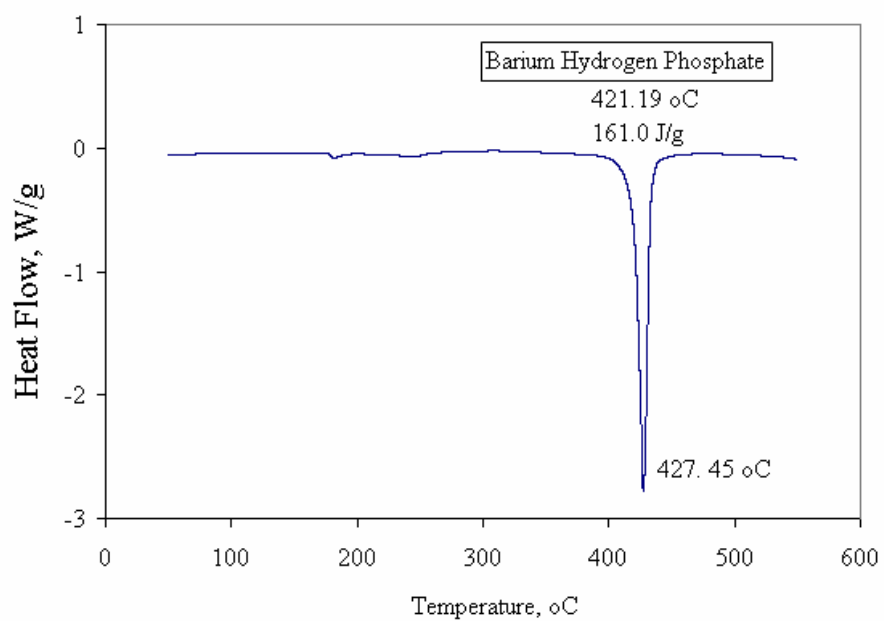


Fig 6.10 DSC Plot of Barium Hydrogen Phosphate

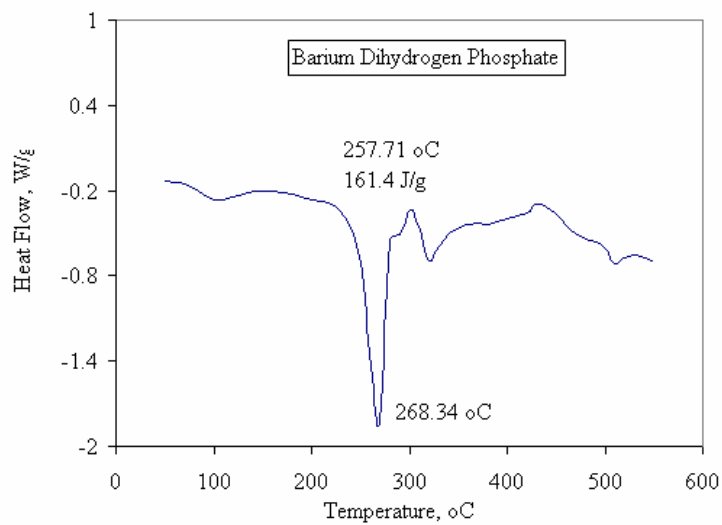


Fig 6.11 DSC Plot of Barium Dihydrogen Phosphate

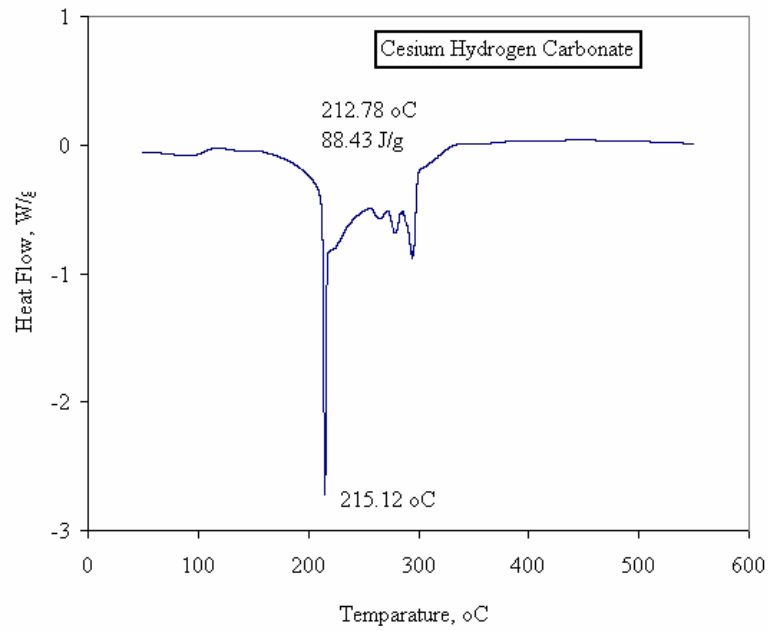


Fig 6.12 DSC Plot of Cesium Hydrogen Carbonate

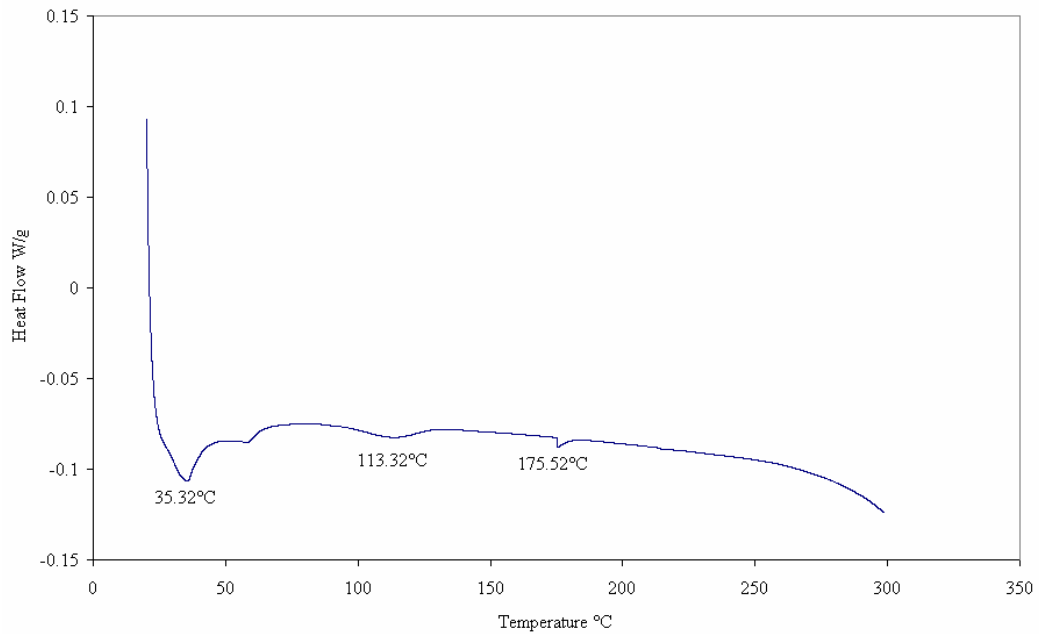


Fig 6.13 DSC Plot of Ammonium Iodide

Table 6.2 DSC Results

Chemical Compound	Phase Transition Temperature
Cesium Hydrogen Sulfate	144.88°C
Barium Hydrogen Phosphate	421.19°C
Barium Dihydrogen Phosphate	268.34°C
Cesium Hydrogen Carbonate	215.12°C
Ammonium Iodide	35.32°C, 113.12°C, 175.52°C

From the DSC plot of Cesium Hydrogen Sulfate it can be inferred that the phase transition temperature for this solid acid electrolyte is 144.88°C which is close to what it is in the literature [4].

### 6.3 X-Ray Diffraction Results

#### 6.3.1 Anchor Scan Parameters

Comment	z=7.650 mm
Measurement Date / Time	10/26/2004 3:07:14 PM
Operator	Sesha
Raw Data Origin	XRD measurement (*.XRDML)
Scan Axis	Gonio
Start Position [°2Th.]	5.0100
End Position [°2Th.]	74.9900
Step Size [°2Th.]	0.0200
Scan Step Time [s]	0.5000
Scan Type	Continuous
Offset [°2Th.]	0.0000
Divergence Slit Type	Fixed
Divergence Slit Size [°]	0.4785
Specimen Length [mm]	10.00
Receiving Slit Size [mm]	0.2500
Measurement Temperature [°C]	25.00
Anode Material	Cu
Generator Settings	45 kV, 40 mA
Goniometer Radius [mm]	320.00
Dist. Focus-Diverg. Slit [mm]	91.00
Incident Beam Monochromator	No
Spinning	No

### 6.3.2 X-Ray Diffraction Pattern of CsHSO<sub>4</sub>

The x-ray diffraction pattern of CsHSO<sub>4</sub> is shown in figure 6.13.

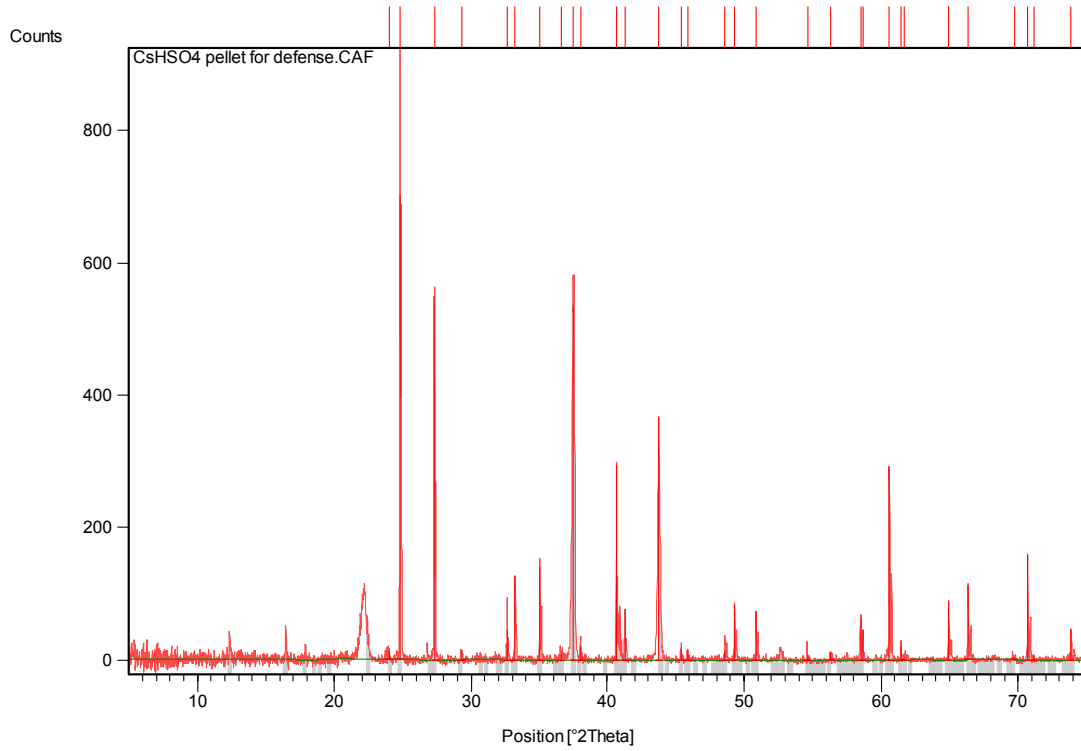


Fig 6.14 X-Ray Diffraction Pattern of CsHSO<sub>4</sub>

### 6.3.3 Peak List

The peak list for the x-ray diffraction pattern of CsHSO<sub>4</sub> is shown in table 6.3.

Table 6.3 Peak List for the X-Ray Diffraction Pattern of CsHSO<sub>4</sub>

Pos. [°2Th.]	Height [cts]	FWHM [°2Th.]	d-spacing [Å]	Rel. Int. [%]	Tip width [°2Th.]	Matched by
23.9849	12.06	0.1181	3.71030	1.72	0.1200	01-082-2214
24.7996	702.65	0.0984	3.59023	100.00	0.1000	01-082-2214
27.2923	563.52	0.0787	3.26772	80.20	0.0800	01-082-2214
29.2677	13.99	0.1181	3.05151	1.99	0.1200	01-082-2214
32.6416	45.82	0.1574	2.74340	6.52	0.1600	01-082-2214
33.2072	127.86	0.0787	2.69796	18.20	0.0800	01-082-2214
35.0055	140.11	0.0480	2.56125	19.94	0.0400	01-082-2214
36.6200	8.75	0.2362	2.45398	1.24	0.2400	01-082-2214

Table 6.3 Continued

37.5427	532.84	0.1574	2.39576	75.83	0.1600	01-082-2214
38.0610	19.56	0.1181	2.36432	2.78	0.1200	01-082-2214
40.6655	293.38	0.0720	2.21687	41.75	0.0600	01-082-2214
41.2906	76.36	0.0787	2.18655	10.87	0.0800	01-082-2214
43.7619	364.98	0.0720	2.06692	51.94	0.0600	01-082-2214
45.4000	16.16	0.1181	1.99773	2.30	0.1200	01-082-2214
45.8593	15.72	0.0960	1.97715	2.24	0.0800	01-082-2214
48.5805	12.59	0.1574	1.87412	1.79	0.1600	01-082-2214
49.3028	83.84	0.0720	1.84681	11.93	0.0600	01-082-2214
50.8687	73.75	0.0720	1.79358	10.50	0.0600	01-082-2214
54.6267	8.03	0.1920	1.67874	1.14	0.1600	01-082-2214
56.2833	12.54	0.0960	1.63319	1.78	0.0800	01-082-2214
58.5044	61.88	0.0720	1.57637	8.81	0.0600	01-082-2214
58.6616	46.42	0.0720	1.57252	6.61	0.0600	01-082-2214
60.6110	291.63	0.0720	1.52652	41.50	0.0600	01-082-2214
61.4415	21.98	0.0720	1.50786	3.13	0.0600	01-082-2214
61.6638	2.54	0.5760	1.50296	0.36	0.4800	01-082-2214
64.9275	88.28	0.0960	1.43507	12.56	0.0800	01-082-2214
66.3548	114.41	0.0960	1.40762	16.28	0.0800	01-082-2214
69.7184	2.52	0.2880	1.34771	0.36	0.2400	01-082-2214
70.6958	159.80	0.0720	1.33145	22.74	0.0600	01-082-2214
71.1465	6.11	0.0720	1.32412	0.87	0.0600	01-082-2214
73.8739	44.99	0.0960	1.28183	6.40	0.0800	01-082-2214

### 6.3.4 Identified Pattern List

The identified pattern list for the x-ray diffraction pattern of CsHSO<sub>4</sub> is shown in table 6.4

Table 6.4 Identified Patterns List for the X-Ray Diffraction Pattern of CsHSO<sub>4</sub>

Visible	Ref. Code	Score	Compound Name	Displacement [°2Th.]	Scale Factor	Chemical Formula
*	01-082-214	35	Cesium Hydrogen Sulfate	0.000	0.190	Cs ( H S O <sub>4</sub> )

### 6.3.5 Plot of Identified Phases

The plot of identified phases for the x-ray diffraction pattern of CsHSO<sub>4</sub> is shown in figure 6.14

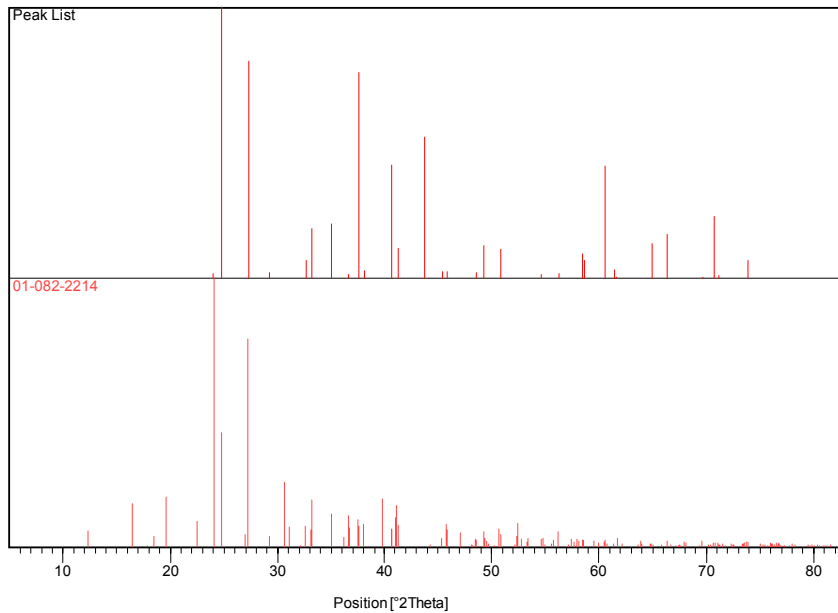


Fig 6.15 Plot of Identified Phases

### 6.4 Infrared Spectroscopy Results

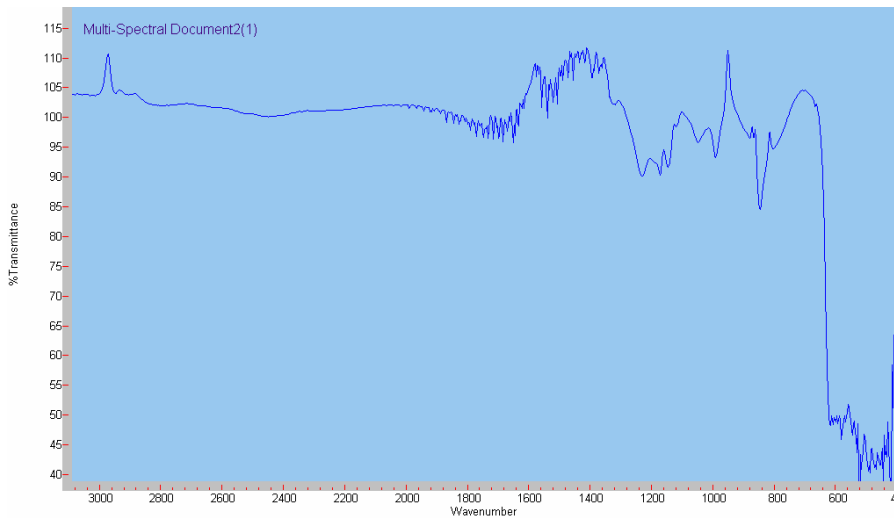


Fig 6.16 Infrared Spectroscopy Results of CsHSO<sub>4</sub> Prepared from Cesium Sulfate

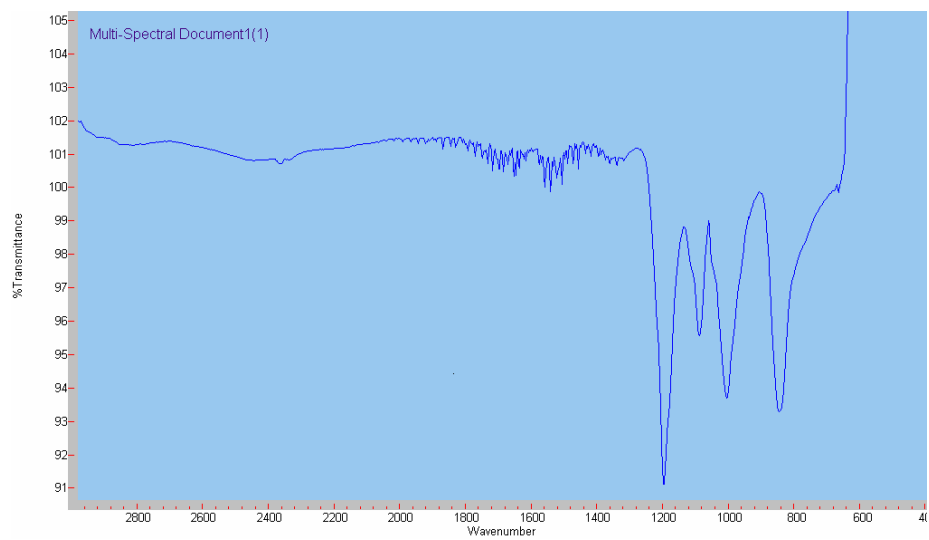


Fig 6.17 Infrared Results of  $\text{CsHSO}_4$  Prepared from Cesium Carbonate



## CHAPTER 7

### SUMMARY AND CONCLUSIONS

The main objective of the thesis was to develop a solid electrolyte for producing hydrogen by electrolysis of hydrogen sulfide. Of these potential electrolytes the main focus was on Cesium Hydrogen Sulfate because of its superprotonic phase transition at 140-150°C. CsHSO<sub>4</sub> was prepared from two chemical compounds namely cesium sulfate and cesium carbonate. Further a die, punch and a base were designed and fabricated in each of two sizes to prepare 0.5” and 2.0” diameter pellets to study the chemical and structural properties of CsHSO<sub>4</sub>. Based on the experimental data one can arrive at the following conclusions:

- CsHSO<sub>4</sub> exhibited a superprotonic phase transition at 140-150°C with a spectacular change in conductivity from 10<sup>-6</sup> to 10<sup>-2</sup> Ω<sup>-1</sup>cm<sup>-1</sup> from impedance measurements.
- Differential Scanning Calorimetry results revealed that the phase transition temperature of CsHSO<sub>4</sub> was between 140°C and 145°C which is in agreement with the literature [4].
- The bond environment of the CsHSO<sub>4</sub> compound was investigated by infrared spectroscopy. The infrared spectrum obtained closely resembles to that in literature [24].

- X-Ray diffraction methods were exclusively used to identify the phases of the  $\text{CsHSO}_4$  compound and the peaks obtained were identified with the reference peaks available in the library of the x-ray diffractometer.
- A successful electrolysis of steam at  $150^\circ\text{C}$  was achieved with the  $\text{CsHSO}_4$  electrolyte.
- Differential Scanning Calorimetry was performed on Barium Hydrogen Phosphate, Barium Dihydrogen Phosphate, Cesium Hydrogen Carbonate, and Ammonium Iodide to identify the thermal transitions of these compounds.

The observed properties of the prepared  $\text{CsHSO}_4$  suggest a favorable prospect for its use in electrochemical dissociation of hydrogen sulfide.

## CHAPTER 8

### RECOMMENDATIONS FOR FUTURE WORK

During the concluding stages of this thesis work there were numerous possibilities for improvement in the results which could not be pursued due to lack of time. There are minor discrepancies in the experimental data between the published values and those reported in this thesis work. The discrepancies can be attributed to a variety of reasons. The highest conductivity value achieved in this thesis research is lower than the highest value published. The decomposition/melting temperature obtained by DSC is higher than the one reported in technical papers. In spite of these minor discrepancies the results attained through this research are encouraging. The following tasks are recommended as future work for improvisation on the results obtained so far:

- The recipe adopted for preparing CsHSO<sub>4</sub> electrolyte needs certain modifications and concrete steps need to be taken to prevent moisture absorption by the electrolyte.
- The thickness of the electrolytes currently used is approximately 1mm. This thickness needs to be decreased further to ensure less electrolyte resistance.
- The pelletization of the chemical compounds should be carried out in a controlled atmosphere and temperature. In order to achieve this vacuum dies may be considered.
- The x-ray diffraction of the CsHSO<sub>4</sub> was performed at room temperature. The same needs to be done at higher temperatures.
- More chemical compounds need to be pursued as potential electrolytes.

## REFERENCES

- [1] A. R. West, *Solid State Chemistry and its Applications*, Chapter 13, Wiley 1984
- [2] Truls Norby, *The Promise of Protonics*, Nature, Volume 410, 19 April, 2001
- [3] S.M. Haile, D.A. Boysen, C.R.I. Chisholm, and R.B. Merle, *Solid acids as fuel cell Electrolytes*, Nature, 410(6831):910–913, 2001
- [4] B. Yang, A. M. Kannan and A. Manthiram, *Stability of the dry proton conductor CsHSO<sub>4</sub> in hydrogen atmosphere*, Materials Research Bulletin, Volume 38, Issue 4, 24 March 2003, Pages 691-698
- [5] L. Kirpichnikova, M. Polomska, J. Wolak and B. Hilczer, *Polarized light study of the CsHSO<sub>4</sub> and CsDSO<sub>4</sub> superprotonic crystals*, Solid State Ionics, Volume 97, Issues 1-4, 1 May 1997, Pages 135-139
- [6] A. V. Belushkin, M. A. Adams, S. Hull and L. A. Shuvalov, *P-T phase diagram of CsHSO<sub>4</sub>. Neutron scattering study of structure and dynamics* Solid State Ionics, Volume 77, April 1995, Pages 91-96
- [7] Xuezhi Ke and Isao Tanaka, *Proton transfer mechanism in solid CsHSO<sub>4</sub> by first-principles study*, Solid State Ionics, In Press, Corrected Proof, Available online 3 July 2004
- [8] A. V. Belushkin, R. L. McGreevy, P. Zetterstrom and L. A. Shivalov, *Mechanism of superprotonic conductivity in CsHSO<sub>4</sub>*, Physica B: Condensed Matter, Volumes 241-243, December 1997, Pages 323-325

- [9] W. Münch, K. D. Kreuer, U. Traub and J. Maier, *Proton transfer in the three-dimensional hydrogen bond network of the high temperature phase of CsHSO<sub>4</sub>: a molecular dynamics study*, Journal of Molecular Structure, Volume 381, Issues 1-3, 31 July 1996, Pages 1-8
- [10] I. N. Levine, *Physical Chemistry*, McGraw-Hill Book Company, New York, 1988
- [11] P. Schuster, G. Zundel, C. Sandorfy, *The Hydrogen Bond*, North-Holland Publishing Company, Amsterdam, 1976
- [12] Calum Ronald Inneas Chisholm, *Superprotonic Phase Transitions in Solid Acids*, California Institute of Technology, December 2002
- [13] Dane Andrew Boysen, *Superprotonic Solid Acids: Structure, Properties, and Applications*, California Institute of Technology, January 9, 2004
- [14] R. E. Hummel, *Electronic Properties of Materials*, Springer-Verlag, New York, 1985
- [15] P. Shewmon, *Diffusion in Solids*, The Minerals, Metals and Materials Society, Warrendale, Pennsylvania, 1989
- [16] Shigenobu Hayashi and Masagi Mizuno, *Proton diffusion in the superprotonic phase of CsHSO<sub>4</sub> studied by <sup>1</sup>H NMR relaxation*, Solid State Ionics, Volume 171, Issues 3-4, 30 July 2004, Pages 289-293
- [17] J. Baran and M. K. Marchewka, *Vibrational investigation of phase transitions in CsHSO<sub>4</sub> crystal*, Journal of Molecular Structure, Volume 614, Issues 1-3, 2 September 2002, Pages 133-149
- [18] Calum R. I. Chisholm and Sossina M. Haile, *X-ray structure refinement of CsHSO<sub>4</sub> in phase II*, Materials Research Bulletin, Volume 35, Issue 7, May 2000, Pages 999-1005

- [19] Masagi Mizuno and Shigenobu Hayashi, *Proton dynamics in phase II of CsHSO<sub>4</sub> studied by <sup>1</sup>H NMR*, Solid State Ionics, Volume 167, Issues 3-4, 27 February 2004, Pages 317-323
- [20] Ae Ran Lim, Jin Hae Chang, Hae Jin Kim and Hyun Min Park, *Phase transition and ferroelastic property studied by using the <sup>133</sup>Cs nuclear magnetic resonance in a CsHSO<sub>4</sub> single crystal*, Solid State Communications, Volume 129, Issue 2, January 2004, Pages 123-127
- [21] Truls Norby, Milan Friesel and Bengt Eric Mallander, *Proton and deuteron conductivity in CsHSO<sub>4</sub> and CsDSO<sub>4</sub> by in situ isotopic exchange*, Solid State Ionics, Volume 77, April 1995, Pages 105-110
- [22] <http://www.psrc.usm.edu/macrog/dsc.htm>
- [23] <http://www.wpi.edu/Academics/Depts/Chemistry/Courses/CH2670/infrared.html>
- [24] Vijay Varma, N. Rangavittal and N. R. Rao, *A study of Superionic CSHSO<sub>4</sub> and Cs<sub>1-x</sub>Li<sub>x</sub>HSO<sub>4</sub> by Vibrational Spectroscopy and X-Ray Diffraction*, Journal of Solid State Chemistry 106, 164-173, 1993